ACCSCIENCE PUBLISHING

International Journal of Bioprinting

REVIEW ARTICLE

Sustainable ALMA from seaweed for DLP printing

Merve Ilgar[1], Eylul Dila Carkci[2], Elif Emekdar[2], Oguzhan Gunduz[3], and Roger Narayan[4]*

[1]Department of Chemistry, İstanbul University-Cerrahpasa, Avcılar, İstanbul, Türkiye

[2]Department of Bioengineering, Yıldız Technical University, Esenler, İstanbul, Türkiye

[3]Department of Metallurgical and Materials Engineering, Marmara University, Maltepe, İstanbul, Türkiye

[4]Department of Biomedical Engineering, North Carolina State University, Raleigh, North Carolina, United States of America

Abstract

Alginate, which can be extracted from various brown seaweed species, is a sustainable biomaterial with several potential biomedical applications because of its biocompatibility and biodegradability. While alginate hydrogels are traditionally ionically crosslinked with divalent cations, this approach often produces hydrogels with low mechanical strength and poorly controlled degradation kinetics, limiting their suitability for biomedical applications. The chemical modification of alginate via methacrylation to produce alginate methacrylate (ALMA) allows the fabrication of photocrosslinkable hydrogels under ultraviolet (UV) light irradiation. This approach enables the fabrication of alginate-based hydrogels with superior physicochemical properties that can be tailored for specific biomedical areas. However, there is a relative lack of research related to the performance of ALMA bioinks in 3D printing using digital light processing (DLP). The research conducted to date indicates a connection between the choice of alginate source, methacrylation chemistry, and printing outcomes. This review directly addresses this topic by considering alginate extraction from brown seaweed, ALMA synthesis methods, and the biomedical applications of ALMA as a 3D hydrogel using DLP. For this purpose, the focus has been on how each step in the process affects the performance of the materials used in final biomedical applications. The goal of this review is to provide researchers with a framework for optimizing ALMA-based bioinks for DLP-based biomedical fabrication.

Keywords: Brown seaweed; Alginate; Extraction methods; Bioink; Digital light processing; ALMA hydrogels

***Corresponding author:**
Roger Narayan
(rjnaraya@ncsu.edu)

Citation: Ilgar M, Carkci ED, Emekdar E, Gunduz O, Narayan R. Sustainable ALMA from seaweed for DLP printing. *Int J Bioprint.* 2026;12(5):026330354.
doi: 10.36922/IJB026330354

Received: June 29, 2026

Revised: August 10, 2026

Accepted: August 19, 2026

Published online: August 21, 2026

Copyright: © 2026 Author(s). This is an Open-Access article distributed under the terms of the Creative Commons Attribution License, permitting distribution, and reproduction in any medium, provided the original work is properly cited.

Publisher's Note: AccScience Publishing remains neutral with regard to jurisdictional claims in published maps and institutional affiliations.

1. Introduction

Marine-derived biopolymers have attracted attention from the research community for their potential use across a wide range of applications, including food packaging, water treatment, energy storage, drug delivery, and tissue engineering.[1-4] The increased interest in these materials can be attributed to their superior characteristics, including biocompatibility, biodegradability, availability, and sustainability.[5] Alginate is a key

component in this category, which is sourced from various brown seaweed species, including *Laminaria digitata, Laminaria hyperborea*, *Macrocystis pyrifera*, *Sargassum* spp., and *Ascophyllum nodosum*.[6] It is one of the most thoroughly studied marine biomaterials in the scientific literature. Structurally, the polymer is built from β-D-mannuronic acid (M) and α-L-guluronic acid (G) units joined by 1→4 glycosidic bonds, and it can constitute up to 40% of the dry weight of brown seaweed.[7,8] The chemical and physical characteristics of alginate, including molecular weight, viscosity, and M/G ratio, depend on the brown seaweed species, harvesting time, and geographical region.[7,9,10] Alginate can form gels via ionic crosslinking with divalent cations, a property that has generated significant interest in this material for biomedical research. However, this crosslinking mechanism is also a major limitation of alginate. Hydrogels formed by this approach often exhibit poor mechanical strength and unpredictable degradation kinetics, limiting their utility in mechanically demanding or in situ applications.[11] To bridge this gap, several chemical functionalization strategies have emerged, and methacrylation has proven to be one of the most effective strategies. When methacrylate groups are added to the alginate backbone, the resulting alginate methacrylate (ALMA) becomes photocurable. Exposure to ultraviolet (UV) light triggers free radical polymerization and forms covalent crosslinks in place of the relatively fragile ionic bonds.[12,13]

The mechanical properties, pore size, swelling, and degradation properties of ALMA hydrogels can be controlled by adjusting the degree of substitution (DS), photoinitiator, UV exposure time, and rheological properties; this approach allows for significant modification of hydrogel properties to meet application-specific requirements.[14] In addition to the ability to adjust and improve these properties, *in situ* gel formation is also possible via the methacrylation process. Thus, ALMA hydrogels can be utilized in biomedical applications such as cell encapsulation, injectable therapeutics, and surgical procedures.[15]

The photocrosslinkable characteristics of ALMA make it compatible with high-resolution additive manufacturing. Because crosslinking can be performed layer-by-layer with UV light via three-dimensional (3D) printing based on digital light processing (DLP), this approach is considered appropriate for building complex ALMA hydrogel designs. Although the use of DLP for biomaterial fabrication is not new, its application to ALMA bioinks has not been examined systematically. This review addresses this underexplored topic. This review considers alginate extraction from brown seaweed and the physicochemical characteristics of the material. It also considers methacrylation strategies and mechanisms for converting alginate into photocrosslinkable bioinks. This review also describes bioink optimization and DLP-based 3D printing of ALMA hydrogels. It subsequently considers the biomedical applications enabled by the combination of these materials and methods. This review concludes by evaluating the current state of the field and future efforts to enhance the functionality of alginate-based hydrogel systems.

2. Alginate extraction methods

Alginate is produced from several brown seaweed species that are harvested from a variety of marine habitats. Within the cell walls of brown seaweed, alginate is not present in a free form. It exists as insoluble salts of calcium, magnesium, sodium, and potassium; these must be removed and the material purified before the polymer can be used.[8] Extraction approaches fall broadly into two categories: conventional chemical protocols and a growing array of green alternatives, including extrusion-based, microwave-assisted, and ultrasound-assisted techniques.[8,16-19] Although the most well-known and widely used method is the conventional chemical method, it requires large amounts of water and chemicals for extraction. Therefore, interest in green alternatives with fewer byproducts and higher yields has increased.[20] The extraction technique and synthesis parameters significantly influence the chemical structure and physicochemical properties of alginate. These attributes determine the degree of substitution (DS) achievable during subsequent methacrylation and, in turn, the rheological behavior of the final ALMA hydrogel.

2.1. Conventional extraction

Among all extraction strategies, the conventional chemical method remains the most extensively employed at both laboratory and industrial scales. This method requires a lengthy amount of time as well as the use of significant amounts of water and chemicals.[8,21] By optimizing the synthesis parameters, the extraction yield of the alginate and its physicochemical properties such as molecular weight, intrinsic viscosity, and M/G ratio (mannuronic acid to guluronic acid ratio) can be adjusted. In this process, the alginate in the brown seaweed cell walls is first converted into its soluble sodium salt form, and the resulting solution is then purified through sequential acid and alkaline treatments. In practice, the seaweed is first exposed to hydrochloric acid (HCl) or calcium chloride ($CaCl_2$), which disrupts the cell wall structure; this step is followed by alkaline extraction with sodium carbonate (Na_2CO_3).[22] The alginate is ultimately recovered by precipitation with an alcohol such as ethanol or isopropanol.[22]

Brown seaweed can be pretreated with a formaldehyde solution to improve the purity of the extract. In this step, the phenolic compounds present in seaweed react with formaldehyde to form insoluble residues, which are then removed during acid treatment.[8] Phenolic components can reduce the intrinsic viscosity of alginate; adding a formaldehyde step to bind these phenolics increases the intrinsic viscosity of the extracted polymer.[23] Therefore, pretreatment with formaldehyde is an important step for adjusting the intrinsic viscosity of alginate.

In the step of forming alginate salts with acid, HCl or $CaCl_2$ is used to form alginic acid or calcium alginate. In general, precipitation with $CaCl_2$ is preferred because it is rapid and yields a fibrous structure. However, an additional process, such as an acid bath, is required to remove calcium. This process can lead to the breaking of polymer chains, resulting in lower molecular weight and viscosity.[24] While using HCl for direct precipitation can be performed in one step, it usually results in lower yields than the $CaCl_2$ method because of material loss in the gel structure.[9,25]

Alkaline extraction is an important step that transfers alginate to the solution and is typically performed using Na_2CO_3, which raises the pH to the extraction conditions.[25] In this step, the pH of the medium should be approximately 10 to prevent damage to the alginate polymer chains. An excessive increase in pH can cleave the β-glycosidic bonds in alginate molecules, leading to the formation of monocarboxylic and dicarboxylic acids.[9] The damaged polymer chains significantly reduce extraction efficiency. As such, if more than 5% Na_2CO_3 is used during alkaline extraction, the efficiency may decrease.[26] The final step in alginate extraction is alcohol precipitation, in which ethanol or isopropanol is added to the sodium alginate solution to precipitate alginate as a fibrous structure. The final alginate is obtained by washing and drying (Figure 1).

2.2. Green extraction

There is a growing interest in developing more sustainable methods for extracting alginate from seaweed, characterized by reduced energy, water, and chemical consumption, as well as shorter reaction times. To address this issue, new production methods, such as extrusion-, microwave-, and ultrasound-assisted alginate extraction, have been developed, as shown in Figure 2.

The extrusion-assisted method, developed as an alternative to conventional batch extraction, facilitates continuous alginate extraction, significantly reducing the extraction time from hours to minutes and halving the requirements for reactants and water.[27,28] In this method, large-scale alginate extraction is achieved using a twin-screw extruder; the screw speed, flow rate, and mold shape can be adjusted.[28,29] Research involving *Laminaria digitata* has demonstrated that alginate extraction via an extruder results in a 7% increase in yield compared to the batch reaction method. Additionally, this approach requires 2.5 times less reactants and water than the conventional method.[27] However, the equipment costs and energy consumption are higher than those of traditional methods,

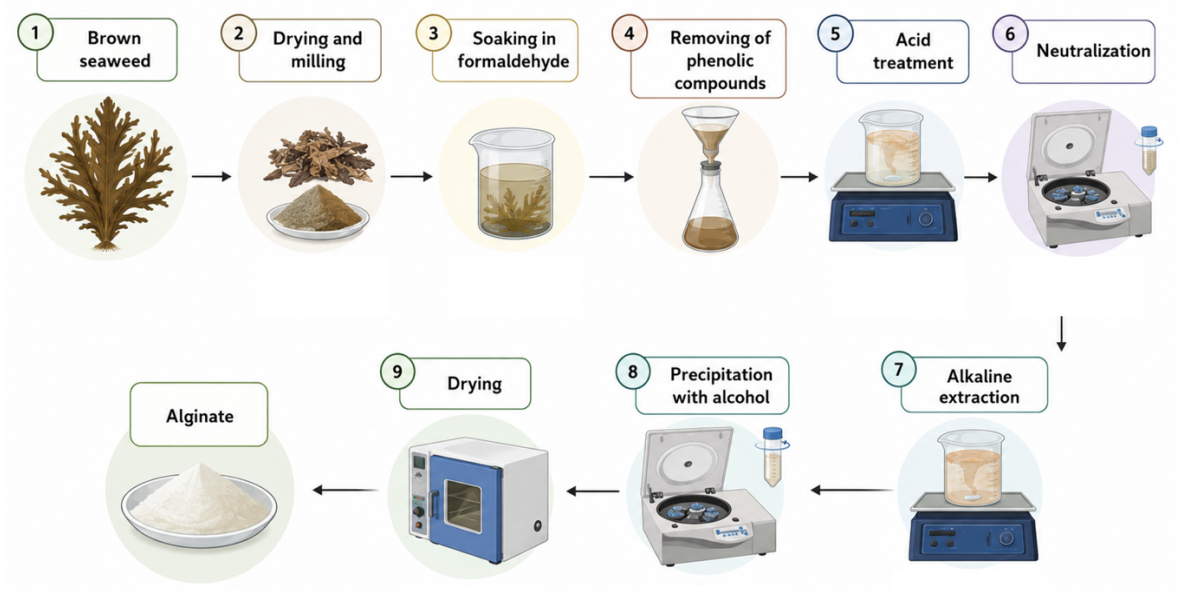


Figure 1. Conventional method steps for sodium alginate extraction from brown seaweed. Schematic created with BioRender. Ilgar, M. (2026) https://BioRender.com/tlur1pt

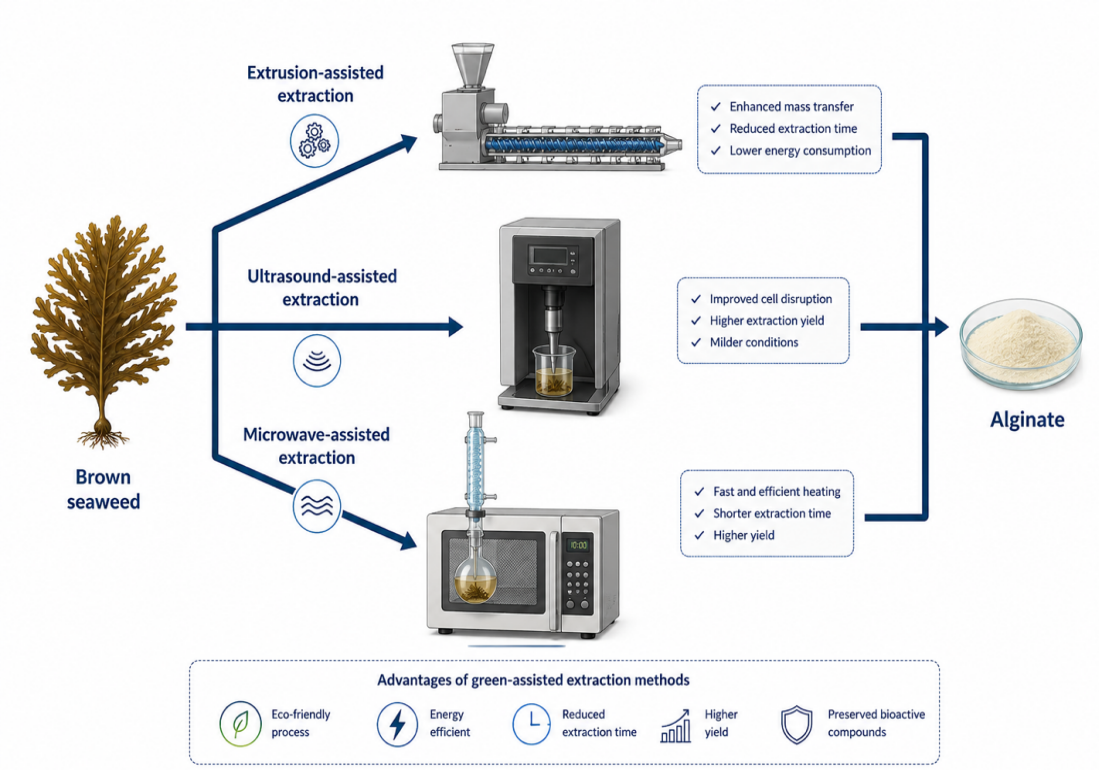


Figure 2. Alginate extraction from brown seaweed using green extraction methods. Schematic created with BioRender. İlgar, M. (2026) https://BioRender.com/fzhe9ic

and this method has not been tested on different types of brown seaweed.

Ultrasound-assisted extraction is a sustainable method that requires minimal solvents, chemicals, and energy, is straightforward to use, and provides rapid results.[8,30] High-intensity ultrasound physically breaks down the cell walls of plant tissue within seconds through the generation of acoustic cavitation. This cavitation allows polysaccharides to be released and dissolved in the cell wall of brown seaweed. Therefore, the extraction efficiency and speed are significantly improved compared to conventional methods. Ultrasound-assisted extraction can preserve the molecular integrity of polymers under optimal conditions.[30] This method enables alginate recovery from the waste seaweed mass remaining after the extraction of other biomolecules such as fucoidan. The alginate yield depends on ultrasound frequency, amplitude, temperature, extraction time, and liquid-solid properties.[19] In a study conducted on *Laminaria digitata*, combining conventional alginate extraction with a 30-minute ultrasound-assisted HCl pretreatment yielded a 30.9% efficiency.[31] Another study found that *Sargassum binderi* and *Turbinaria ornata* produced a yield of 55% of their dry weight within 15 to 30 minutes, whereas traditional extraction methods resulted in a 27% yield after 2 hours.[32] Although this method allows for the high-yield production of alginate with short extraction times, ultrasonic waves tend to reduce the molecular weight of the alginate. Sonication can break glycosidic bonds in the middle of the chain, leading to a decrease in molecular weight.[33] Sonication time plays an important role in shaping the molar mass, block structure, and rheological behavior of alginate. Compared to conventional and other green extraction techniques, ultrasonically extracted alginate consistently exhibits lower molecular weight and viscosity.[16,33] This is a desirable outcome when a low-viscosity alginate formulation is required; however, it remains a limitation for applications in which high viscosity is required.

In addition to ultrasound-based approaches, microwave-assisted extraction of alginate from brown seaweed enhances the reaction process by facilitating the rapid and efficient heating of solvents, thereby reducing the need for chemical solutions. The thermal energy produced by microwaves causes the evaporation of water within seaweed cells, leading to increased pressure on the cell walls. This pressure effectively ruptures the cell

walls, thereby releasing intracellular compounds into the extraction solvent.[34] Several factors influence the efficiency of microwave-assisted extraction, including microwave power and frequency, extraction duration, solvent concentration, matrix characteristics, solid-liquid ratio, pressure, extraction cycles, solvent properties, and temperature.[35] In a study on the extraction of alginate from *Undaria pinnatifida*, microwave-assisted extraction was performed at 91.86 °C for 15 minutes, resulting in a yield of 38.41%.[36] In another study, alginate was obtained from the brown seaweed species *Sargassum cristaefolium* with a yield of 40.6% under synthesis conditions of 80 °C for 20 minutes.[37] Compared to extraction protocols that require hours, microwave treatment is significantly faster, uses less energy, and is more cost-effective. However, rapid microwave-alkali extraction has not been systematically compared across a broader range of brown seaweed species; most optimization studies to date have focused narrowly on a single species.[36] Nevertheless, green alginate extraction techniques are promising in terms of yield, short extraction time, as well as reduced solvent and chemical use compared to traditional methods. Table 1 summarizes the reported representative yield, molecular weight, and M/G ratio values for alginate obtained from various brown seaweed species using conventional, ultrasonic, microwave, and extrusion-based methods, and demonstrates how species

Table 1. Physicochemical properties of alginate material that was extracted from brown seaweed species in various marine regions

Species	Region	Extraction method	Extraction conditions	Yield (%)	Average molecular weight (kDa)	M/G ratio	Ref.
Sargassum latifolium	Egypt, Red Sea Coast	Conventional	1.5% (w/v) seaweed in 3% Na_2CO_3; 1–3 hours at 25–45°C	18–40	141–213	0.94–2.70	10
Sargassum muticum	Praia da Mourisca, Pontevedra, Spain	Ultrasound	20:1 liquid-to-solid ratio; 150 W, 40 Hz; 5–30 minutes at 25°C	5.7–15	80–112	0.33–0.64	16
Cystoseira barbata	Mangalia, Romanian Black Sea	Conventional	3% (w/v) Na_2CO_3; 25 g seaweed; 2 hours at 60 °C	19	126.6	0.64	21
Laminaria digitata	Portsall, Brittany, France	Extrusion	4% (w/w) Na_2CO_3; twin-screw extruder (12 cm diameter, 4-cm magnetic stirrer); 30 minutes	39	105	N/R	27
Laminaria digitata	Ozon Way, Belgrade, Serbia	Ultrasound	HCl pretreatment (40 kHz, 150 W ultrasound) + 3% (w/v) Na_2CO_3, 20 mL/g liquid/ solid ratio for 2 hours at 60 °C	30.9	N/R	1.08	31
Undaria pinnatifida	Seoul, Republic of Korea (commercial)	Microwave	Solid/liquid ratio 13.27 g/L; 2.51% (w/v) Na_2CO_3; 200 W; 91.86 °C; 15 minutes	38.41	N/R	N/R	36
Zonaria sp., *Chnoospora* sp., *Spatoglossum* sp., *Sargassum* sp., and *Sargassum sp.*	Madagascar Coast	Conventional	1 M Na_2CO_3; 2 hours at 60 °C	23.6 / 26.6	113–420.5	0.41–1.09	38
Sargassum vulgare	Lebanese Mediterranean coast, Tripoli	Conventional	0.5 M Na_2CO_3 (1 L per 100 g seaweed); 3 hours at 50 °C	40	110	0.785	39

(*Cont'd...*)

Table 1. (*Continued*)

Species	Region	Extraction method	Extraction conditions	Yield (%)	Average molecular weight (kDa)	M/G ratio	Ref.
Nizamuddinia zanardini	Oman Sea, south of Iran	Conventional	3% (w/v) Na_2CO_3; 25 g seaweed; 2.5 hours at 60 °C	24	103	1.11	40
Sargassum cristaefolium	Poteran Island, Sumenep, Madura, Indonesia	Extrusion	1%–10% (w/v) Na_2CO_3; twin-screw extruder (capacity 7 kg/h; die 8 mm; screw 0-180 rpm; feed 0–35 rpm)	34.96	211.93	0.29	41
Sargassum spp.	Caribbean Region	Conventional	1%–10% (w/v) Na_2CO_3; 5–15 mL Na_2CO_3 per 1 g dried seaweed; 0.5–6 hours at 22–80 °C	28.16	314	0.45	42
Sargassum cymosum C. Agardh	Ubatuba, São Paulo, Brazil	Ultrasound	2% (w/v) Na_2CO_3; 20 kHz; 120–180 W; 5–15 min	10-54	94.28–203.26	0.74	43
Macrocystis pyrifera	British Columbia Coastline, Canada	Conventional	Three protocols compared; 1% $CaCl_2$ + HCl pretreatment + 0.5% Na_2CO_3 alkaline extraction at 45 °C, 30 minutes / 70% ethanol + HCl pretreatment + 3% Na_2CO_3 alkaline extraction at 60 °C, 2 hours / 0.2 M chelate treatment, 16 hours	24.3 / 22.3 / 26.7	241 / 228 / 59.5	1.23 / 1.53 / 0.63	44
Nizamuddinia zanardini	Chabahar, Sistan-Baluchistan, Iran	Conventional / ultrasound / microwave / ultrasound and microwave	Four protocols compared in 10 g of seaweed in 3% (w/v) Na_2CO_3; 6 hours at 65 °C / 20 kHz, 200 W at 55 °C for 15 minutes / 700 W at 90 °C for 15 minutes / ultrasound at 55 °C for 15 minutes and microwave at 90 °C for 15 minutes	11.88 /12.87 /15.36 /13.99	3021 / 2362 /3015 / 2608	N/R	45

Note: N/R: Not reported in the source study.

and extraction conditions determine the physicochemical profile of the resulting polymer.

From a DLP bioprinting perspective, the extraction stage is not only a raw material production step but also a step that affects the bioink performance. The molecular weight, viscosity, and M/G ratio influence the rheological behavior of ALMA, DS yield, and printing accuracy of the final bioink. As such, optimizing alginate extraction is an important step for obtaining high-resolution and dimensionally accurate 3D structures via DLP bioprinting.

3. Chemical structure of alginate

Alginate is a linear, anionic polysaccharide composed of two uronic acid monomers, which are β-D-mannuronic acid (M) and α-L-guluronic acid (G), joined by 1→4 glycosidic linkages, as illustrated in Figure 3. These monomers are organized into stretches of consecutive M units (MM blocks), stretches of consecutive G units (GG

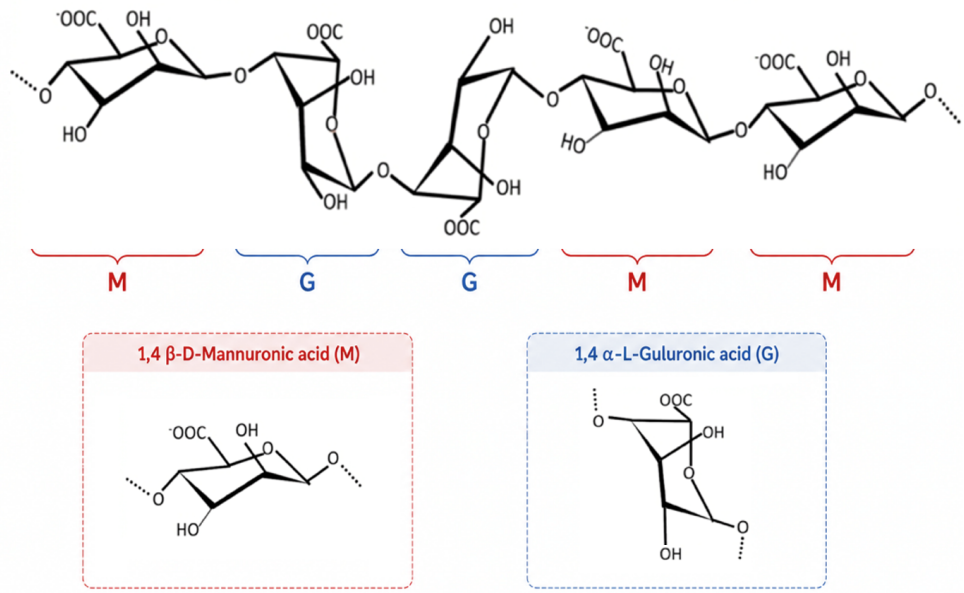


Figure 3. The chemical structure of alginate. Schematic created by the authors using PowerPoint and Gemini

blocks), and mixed alternating sequences (MG or GM blocks), with the proportions of each block type varying considerably across alginate sources, harvest regions, and time.[7,8] The block-level architecture significantly affects material properties, with the M/G ratio being a key factor influencing intrinsic viscosity, gel strength, and the overall elasticity of the hydrogel that is produced.[46] Alginate characterized by a high M/G ratio tends to have a softer chain, attributed to its lower molecular weight and viscosity, resulting from a greater presence of flexible MM content. Conversely, a lower M/G ratio coupled with increased GG content leads to a more rigid chain structure.[10,47] The flexibility of the chains and the overall performance of the polymer are significantly influenced by the arrangement of the MM and GG sites and their density within the alginate polymer structure. Therefore, the precise arrangement of MM and GG sequences along the backbone is not merely a structural detail but instead a functional determinant that governs chain flexibility, crosslinking behavior, and the physicochemical and biological properties exhibited by the final material.

The M/G arrangement of alginate is an important property for DLP printing of ALMA-based bioinks. The differences in the arrangements and M/G ratio affect the yield of DS resulting from ALMA synthesis, thereby influencing the crosslinking behavior of ALMA under the UV-visible light. As such, the molecular structure of alginate contributes to the overall printing properties of the DLP-produced hydrogels.

4. Ionically crosslinked alginate

Alginate is a biopolymer with carboxyl and hydroxyl groups that can form hydrogels via ionic crosslinking with ions such as Ca^{2+}, Ba^{2+}, and Sr^{2+}.[46] In the alginate chain structure, M monomer blocks form weaker bonds with divalent cations, whereas G monomer blocks create an egg-box model that enables the formation of junction regions.[48] This process results in the formation of a stable hydrogel network with pore sizes of 5–200 nm and high porosity in the alginate containing high G-blocks.[49,50] Upon exposure to water, hydrogels swell via their pores; this characteristic is exploited in biomedical applications (e.g., drug delivery and tissue engineering).[51] The solubility and gelation characteristics of alginate are influenced by pH levels. A decrease in pH results in the protonation of carboxyl groups, rendering alginate insoluble in acidic environments.[52] The pH sensitivity of alginate is beneficial, especially in drug delivery systems, as a high pH promotes rapid release, whereas a low pH inhibits rapid release.[41,53] The gel-forming, pH-sensitive, and swelling properties of alginate, along with its biocompatibility, make it a widely used material in biomedical applications.[35] However, ionically crosslinked alginate hydrogels exhibit poor mechanical properties and limited *in vivo* stability. Therefore, chemical modification of alginate is necessary to produce mechanically robust, geometrically defined constructs, which are preformed *in vitro* before *in vivo* use.[13] These shortcomings become more pronounced in DLP-based manufacturing; in this approach, the material

must maintain its geometry throughout the layer-by-layer photopolymerization process. Because this is not possible for hydrogels via ionic crosslinking alone, 3D structures with structural integrity can be produced with DLP through the chemical modification of alginate. The ionic and covalent crosslinking of alginate is schematically illustrated in Figure 4.

5. Alginate methacrylate (ALMA)

5.1. Synthesis methods of ALMA

Although ionically crosslinked alginate is naturally biocompatible, exhibits low toxicity, and is widely used, it lacks sufficient structural stability for many applications. This limitation can be overcome by covalently crosslinking alginate, which forms a permanent network that is more stable than ionic crosslinking and less susceptible to degradation under physiological conditions.[54] Because alginate contains carboxyl (-COOH) and hydroxyl (-OH) groups, it is compatible with various covalent modifications, such as esterification, amidation, oxidation, succinylation, and acetylation.[55] Among these modification techniques, methacrylation is the most used method for alginate modification via esterification or amidation. In the synthesis of ALMA, UV-curable ALMA

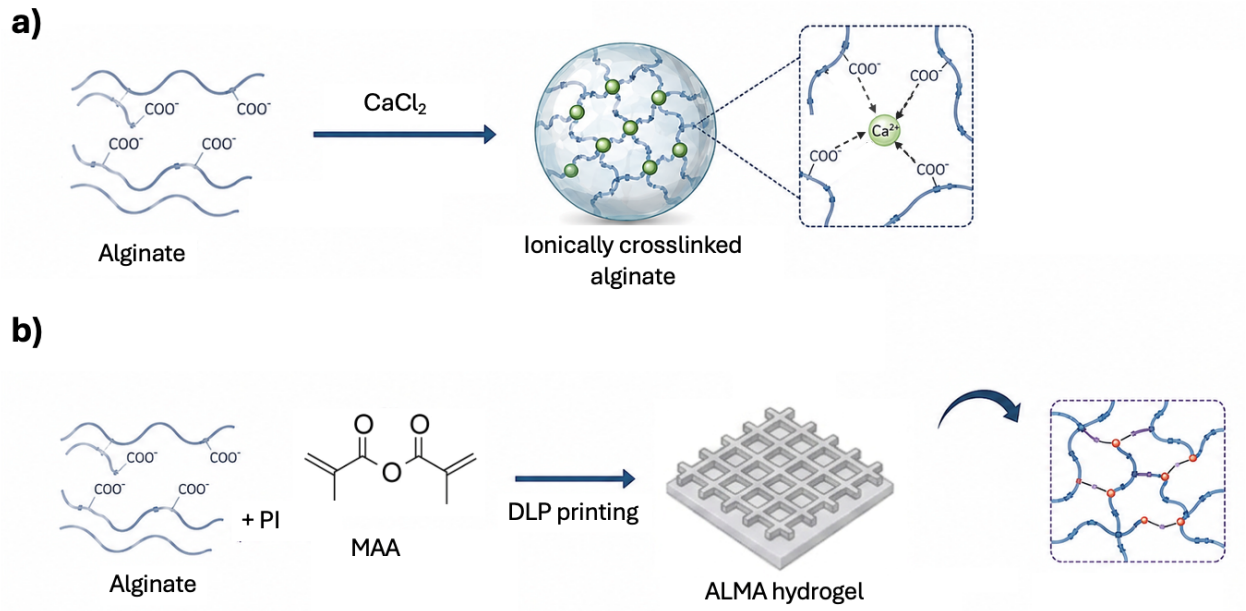


Figure 4. Ionic and covalent strategies for alginate hydrogels. (a) Ionically crosslinked alginate microbeads, and (b) 3D ALMA hydrogel fabrication using a 3D DLP printer.
Abbreviations: ALMA: alginate methacrylate; DLP: Digital light processing; MAA: Methacrylic anhydride; PI: Photoinitiator. Schematic created by the authors using PowerPoint and Gemini.

hydrogels are formed by incorporating methacrylate groups into the alginate chain backbone. The DS value of ALMA represents the number of methacrylate groups in the alginate backbone.[14] As DS directly affects swelling behavior, elastic modulus, and degradation rate, its precise adjustment during synthesis is an important parameter.[56] In DLP 3D printing, the DS value determines the print resolution, layer adhesion, and mechanical properties of the final hydrogel. Therefore, careful adjustment of the DS value is essential during the design stage.

The DS value of ALMA can be controlled by synthesis conditions such as reaction time, temperature, concentration, pH, and modification method. The toxicity, biodegradability, and mechanical properties of the resulting materials can be effectively controlled by adjusting these parameters. In the most reported route, MAA reacts with alginate in a single-step esterification to introduce methacryloyl groups; the resulting carbon-carbon double bonds subsequently enable radical-initiated photocrosslinking.[57] MAA reacts with the hydroxyl groups of alginate via esterification.[58] Methacrylation of alginate using MAA, as illustrated in Figure 5, involves the addition of MAA to alginate in a phosphate-buffered saline (PBS) solution at room temperature (RT); the pH value is

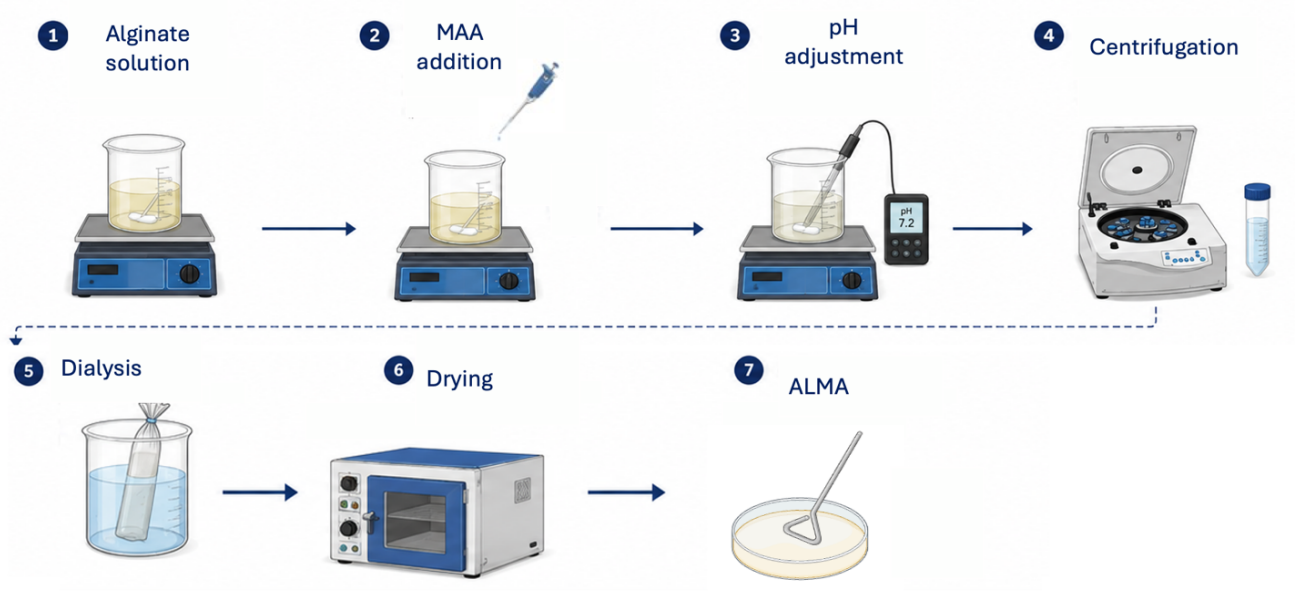


Figure 5. ALMA synthesis steps with MAA
Abbreviations: ALMA: alginate methacrylate; MAA: Methacrylic anhydride. Schematic created with BioRender. İlgar, M. (2026) https://BioRender.com/fzhe9ic

adjusted with sodium hydroxide (NaOH). The reaction is allowed to proceed for 8–24 hours, after which the product is precipitated with ethanol or acetone, dialyzed, and freeze-dried.[15] During methacrylation, the hydrolysis of MAA leads to the formation of methacrylic acid as a byproduct, causing a rapid decrease in pH; therefore, maintaining an alkaline pH throughout the synthesis process is essential. Moreover, variables such as the rate at which MAA is added, reaction temperature, pH, and other mixing conditions can significantly affect the homogeneity and quality of the reaction, ultimately influencing the DS value of ALMA.[58,59]

In the 2-aminoethyl methacrylate (AEMA) modification process, the carboxyl groups of alginate are first activated with 1-ethyl-3-(3-dimethylaminopropyl)-carbodiimide hydrochloride (EDC)/N-hydroxysuccinimide (NHS), after which AEMA reacts with the activated carboxyl groups to form amide bonds.[56] The reaction is carried out in a buffered solution, such as 2-(N-morpholino)ethanesulfonic acid (MES), at room temperature for 24 hours, after which the product is precipitated with an organic solvent, such as acetone, dialyzed, and freeze-dried.[60] Despite this complexity, AEMA remains attractive because the DS value can be precisely controlled by adjusting the amount of AEMA added to the reaction. If the DS is increased, the elastic modulus of the resulting hydrogel increases, while the pore size decreases. Another advantage is that some carboxyl groups remain unreacted and are therefore available for further functionalization (e.g., with RGD peptides to promote cell adhesion).[59] The approach does, however, present challenges, such as a complex procedure (e.g., the EDC/NHS activation step) and high cost.[59]

Glycidyl methacrylate (GMA) exhibits its own, sometimes unpredictable, reaction chemistry. The reagent can modify alginate through two pathways: transesterification at hydroxyl sites or epoxide ring-opening at carboxyl sites; controlling the dominant pathway is not always straightforward.[59] The synthesis is accomplished by adding GMA to an alginate solution adjusted to approximately pH 10, allowing the reaction to proceed at approximately 60 °C for 4–6 hours, and then purifying the product by ethanol precipitation and lyophilization.[13] ALMA produced by this method can undergo thermal polymerization at body temperature when used with suitable initiators (e.g., ammonium persulfate [APS] and tetramethylethylenediamine [TEMED]). Thus, hydrogels that can form gels at physiological temperatures can be produced. In this context, ALMA, which is injected directly into the target area, offers a practical solution for surgical applications by rapidly gelling at body temperature.[13] Although GMA is an economical solution that can be thermally cured, the fact that the reaction proceeds in two different ways limits the reproducibility and controlled production of the final product.[59] Figure 6 shows ALMA

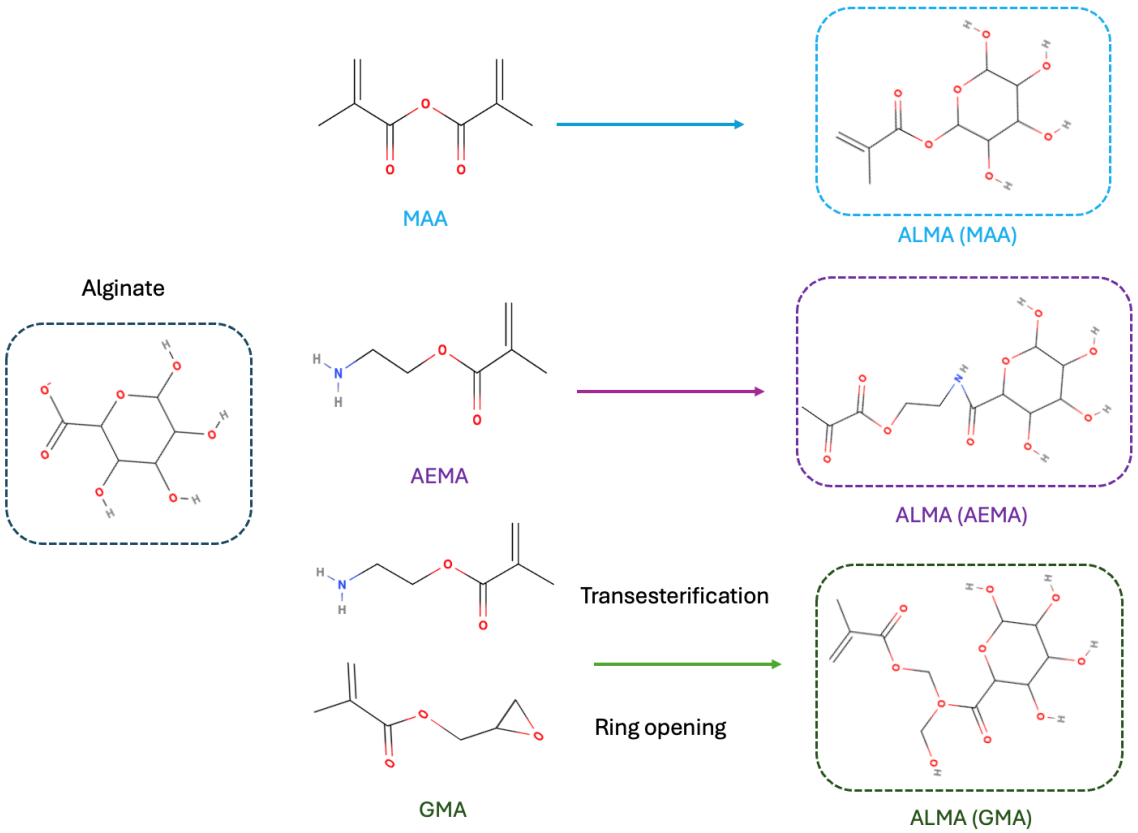


Figure 6. ALMA synthesis using MAA, AEMA, and GMA
Abbreviations: AEMA: 2-aminoethyl methacrylate; ALMA: alginate methacrylate; GMA: Glycidyl methacrylate; MAA: Methacrylic anhydride. Schematic created by the authors using Mind the Graph and PowerPoint.

synthesis reactions using MAA, AEMA, and GMA, each of which offers distinct advantages.

When comparing the three approaches, the MAA method stands out for its procedural simplicity; it is the most widely used method. Although GMA-modified alginate can be crosslinked *in situ*, which is advantageous for certain applications, its dual reaction pathway yields an inconsistent DS and therefore poses a reproducibility problem. AEMA falls between the two in terms of cost and complexity, but it is a more stable and tunable synthesis method than the other methods. However, these three methods have not been compared in a comprehensive manner. A systematic comparison would help demonstrate which method is most suitable for a given biomedical application.

5.2. Properties of ALMA

Due to its covalent network structure, ALMA forms a more stable structure than the egg-box ionic structure of alginate, resulting in more stable mechanical properties.[61] While ionic crosslinked alginate can undergo shape loss due to ion diffusion, in ALMA, the gelation time via photopolymerization can be adjusted by UV exposure time, allowing for the production of the desired geometry and subsequent preservation of the printing geometry.[58,61,62] Additionally, by varying the DS and crosslinking density, the degradation rate of the hydrogel, which is an important parameter for drug delivery and tissue engineering, can be controlled.[61] However, ALMA synthesis requires further purification and nuclear magnetic resonance (NMR) characterization since it involves the modification of alginate with methacrylate groups.[61,62] The chemical materials required for methacrylation, a suitable photoinitiator, a UV light system, and additional characterization are more expensive than those required for ionic crosslinked alginate.[61-63]

The primary characteristics that set ALMA apart from other photocurable biomaterials are its notable advantages in terms of sustainability and functional versatility. ALMA can easily form double networks or interpenetrating polymer networks (IPNs) with other photopolymers such as gelatin methacryloyl (GelMA), polyethylene glycol

diacrylate (PEGDA), and hyaluronic acid methacrylate (HAMA); these combinations enhance the mechanical properties and biological performance of the resulting materials. This strategy is particularly advantageous because each of these biomaterials has intrinsic limitations when used alone. Despite its excellent biocompatibility and bioactivity, GelMA has been reported to have lower toughness than hybrid biopolymers made with ALMA.[64] PEGDA, a synthetic polymer, possesses high mechanical strength, but it lacks inherent bioactivity and must be further modified to achieve it.[65] HAMA, despite its similarity to the extracellular matrix (ECM) and high biocompatibility, has poor mechanical properties and limited cell adhesion, resulting in low 3D print quality and high cost when used alone.[66]

ALMA, unlike other commonly used photocrosslinkable biomaterials, has the advantage of being able to doubly crosslink with divalent cations even after methacrylation of the G blocks in its polysaccharide backbone. This double crosslinking is achieved by first applying rapid ionic gelation, followed by a stable covalent photocrosslinking step. As a result, ionic bonds coexist with a stable covalent backbone through a double-network mechanism, producing hydrogels with greater toughness and tunable stiffness than fully covalently crosslinked biomaterials.[67] Alginate is a low-cost and abundant marine-derived polysaccharide. Unlike gelatin, it is not of animal origin and has a low immunogenicity profile.[59] However, it has a lower DS than GelMA because methacrylation can only be applied to the G units of alginate, resulting in weaker crosslinking and consequently lower mechanical properties.[68] Furthermore, alginate cannot be enzymatically degraded in mammals due to the absence of alginase, leading to uncontrolled calcium ion release.[69] This parameter should be considered for applications where predictable degradation is required. Alginate polysaccharide exhibits poor cell adhesion, which is why ALMA-based inks often need to be mixed with an adhesive polymer such as GelMA or functionalized with RGD peptides to support strong cell adhesion.[59] ALMA has been used in tissue engineering for various functions beyond its utility as a scaffold. The dual crosslinking feature of ALMA has enabled the creation of microfibers and microgels that maintain mechanical stability and retain their 3D structure in physiological conditions, while also supporting tissue growth.[67]

ALMA has also been used as a vehicle for growth factors and drug delivery. A wound dressing with sustained release due to degradation has been developed by covalently binding vascular endothelial growth factor (VEGF) to a methacryloyl-alginate/chondroitin sulfate patch.[70] ALMA is a multifunctional biomaterial capable of contributing to mechanical reinforcement, controlled biodegradation, and localized delivery of bioactive molecules in hydrogel systems. Most ALMA-based systems have been manufactured through extrusion rather than vat photopolymerization. The development of composite formulations that are compatible with DLP, while maintaining their mechanical properties, remains largely unexplored and necessitates further research.

Table 2 provides a comparative overview of how the choice of methacrylate agent, initiator, and concentration affect the DS, cell viability, and mechanical properties.

Table 2. Summary of ALMA hydrogel properties

Methacrylate agent	DS	Hydrogels concentration (% w/v)	Crosslinking method / Photoinitiator	Fabrication	Mechanical properties	Cell type / Viability	Application	Ref.
GMA	25.8	1	APS + TEMED (Thermal, 37 °C)	N/R	N/R	HUVEC; >80%	Potential tissue engineering scaffold applications	13
GMA / AEMA / MAA	31.39 /28.03 /32.35	2 /1 /2	Irgacure 2959 (UV; 365 nm)	Mold casting	15 kPa (Young's modulus)	N/R	N/R	14
MAA	21 /33	2	VA-086 (UV, 365 nm)	Mold casting	2.63 /13.16 kPa (Young's modulus)	N/R	UV-based bioprinting applications	15
AEMA	4.15-25.23	1	Irgacure 2959 (UV, 365 nm)	Mold casting	34.29-174 .77 kPa (Elastic modulus)	Bovine chondrocytes; >80%	Potential cell transplantation and drug delivery	56

(*Cont'd...*)

Table 2. (*Continued*)

Methacrylate agent	DS	Hydrogels concentration (% w/v)	Crosslinking method / Photoinitiator	Fabrication	Mechanical properties	Cell type / Viability	Application	Ref.
MAA	10-33	3	$CaCl_2$ (Ionic) + LAP (UV, 365 nm)	Mold casting	0.27-0.87 MPa (Young's modulus)	N/R	Smart hydrogels for 4D-printing	58
MAA	61.31	1-5	$CaCl_2$ (Ionic) + Irgacure 2959 (UV, 360-480 nm)	Microfluidic fabrication	≈6 MPa (tensile stress)	HUVEC; >85%	Cell-encapsulated microfibers-based scaffolds	67
MAA	8.77	8	LAP (UV, 405 nm)	Extrusion 3D printing	From 1.6 to 2.0–2.6 kPa (Young's modulus)	N/R	Potential in the biomedicine, tissue engineering, and food fields	71
MAA	2.5 /5 /7.5	2 /3	Irgacure 2959 (UV, 368 nm)	Mold casting	0.5850–8.824 kPa (Young's modulus)	Nucleus pulposus cells; high viability	Potential cartilaginous tissue engineering	72
MAA	N/R	2	Eosin Y (Argon ion laser, 514 nm)	Mold casting	N/R	MCF-7 cancer cells	Drug delivery	73
MAA	-	1 / 3	$CaCl_2$ (Ionic) + EY (green light)	Mold casting	16–60 kPa (Elastic modulus)	C2C12 myoblasts; high viability	Hydrogel scaffolds	74
OMA	15.8 /21.5 /28.13	4 /6	$CaCl_2$ (Ionic) + EY (475 nm)	Mold casting	4.85–21.02 kPa (Elastic modulus)	L-929 fibroblast cells; >80%	Potential tissue engineering applications	75
MAA	23.4–53.5	3	Electron beam ALMA + PEGDA	Mold casting	N/R	N/R	Potential wound dressing	76
MAA	N/R	0.5	EY; ALMA + gelatin + silk fibroin	Extrusion 3D bioprinting	N/R	MG-63 human osteosarcoma cell line, high cell proliferation	Cell-laden scaffolds	77
GMA	30-55	2-4	Irgacure 2959; (UV, 312 nm)	Electrospun in the PEO fiber matrix	109 MPa (Young's modulus)	N/R	Potential scaffolds for tissue engineering	78
MAA	11.5	5	Irgacure 2959 (UV at 365 nm) ALMA + EGDA/ EGDMA/TEGDMA	Mold casting	10–50 (kPa Young's modulus)	Human skin fibroblasts; high viability	Potential wound healing	79

Abbreviations: AEMA, 2-Aminoethyl methacrylate; APS: Ammonium persulfate; DS: Degree of substitution; EGDA: Ethylene glycol diacrylate; EGDMA: Ethylene glycol dimethacrylate; EY: Eosin Y; GelMA: Gelatin methacryloyl; GMA: Glycidyl methacrylate; HUVEC: Human umbilical vein endothelial cell; Irgacure 2959: 2-Hydroxy-4′-(2-hydroxyethoxy)-2-methylpropiophenone; LAP: Lithium phenyl-2,4,6-trimethylbenzoylphosphinate; MAA: Methacrylic anhydride; N/R: Not reported; PEGDA: Polyethylene glycol diacrylate; OMA: Oxidized methacrylate alginate; TEGDMA: Triethylene glycol dimethacrylate; TEMED: Tetramethylethylenediamine; VA-086: 2,2'-Azobis[2-methyl-N-(2-hydroxyethyl)propionamide.

5.3. ALMA hydrogels for DLP printing

According to the ISO/ASTM 52900 standard, additive manufacturing is divided into categories such as material extrusion, material jetting, binder jetting, powder bed fusion, directed energy deposition, sheet lamination, and vat photopolymerization.[80,81] Material extrusion is the most commonly used alternative for soft tissue bioprinting because of its ability to operate over a wide viscosity range at a relatively low cost. However, the shear forces generated as the bioink passes through the nozzle can reduce cell viability, and resolution is limited, restricting the production of fine structures for vascular or neural applications.[81] Powder bed fusion, binder spraying, sheet lamination, and directed energy deposition methods have been developed for processing metals, ceramics, thermoplastics, and polymers. Because the techniques operate at high temperatures, they are generally more suitable for cell-free scaffolds and rigid tissue implants.[81] The material spraying method can deposit bioink droplets with good positional accuracy; however, the low viscosity required to prevent nozzle clogging narrows the range of formulations that can be printed.[81] In contrast, vat photopolymerization is particularly important for producing cell-compatible hydrogels because it is associated with the production of high-resolution structures, rapid layer formation, and the ability to create complex internal geometries with relatively low mechanical stress, especially in hydrogel structures with living cells.[82,83] It fundamentally involves curing a photosensitive resin with UV light to construct a 3D scaffold incrementally, layer by layer, from a resin-filled tank.[84] Owing to its biocompatibility and suitability for chemical modification, alginate can be used in tissue engineering to produce complex and cell-loaded 3D structures with high resolution via vat photopolymerization-based printing.[83]

DLP is an additive manufacturing technique that allows for the creation of complex, tailor-made 3D structures. In DLP-based systems, a digital light source, such as UV, blue, visible, or near-infrared (NIR) light, triggers localized free-radical photopolymerization, converting photocrosslinkable liquid resins into solid 3D constructs in a layer-by-layer manner.[85,86] At the molecular level, this process involves the crosslinking of low-molecular-weight monomers and oligomers to ultimately form high-molecular-weight solid-polymer networks.[87] A typical DLP printer comprises several core components: a moving platform, a digital micromirror device (DMD), a UV light source system, a lens assembly, a cuvette for holding the bioink, a high-precision z-axis motion tool, and control software, as shown in Figure 7.[88] Together with its relative ease of use, lower cost than many alternatives, and high-resolution printing, these features make DLP an attractive platform for biomedical manufacturing.[85]

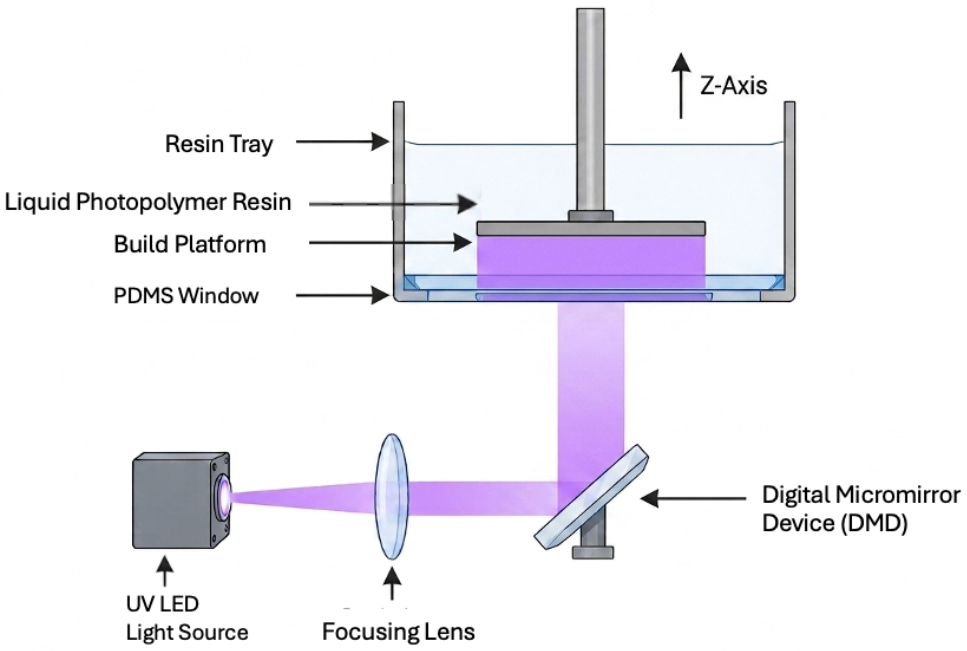


Figure 7. Working principle of DLP 3D printer
Abbreviations: PDMS: Polydimethylsiloxane. Schematic created with BioRender. İlgar, M. (2026) https://BioRender.com/fzhe9ic

Compared with other bioprinting strategies, DLP plays an important role in vat polymerization applications by offering finer control of mechanical properties, lower costs, and excellent cell viability. In contrast to point laser scanning systems, DLP employs a digital micromirror device (DMD) to cure an entire layer using a single light projection. This approach significantly reduces manufacturing time; in addition, it limits the external exposure and stress experienced by the cells.[89] Consequently, DLP effectively converts alginate-based structures into micrometer-scale tissue scaffolds with a resolution scalable to approximately 1 μm, making it a highly attractive platform for biomedical manufacturing.[85,89]

To produce DLP-printed hydrogels with the desired mechanical properties and biocompatibility, a suitable photocrosslinkable bioink is required. A variety of DLP bioinks have been developed by functionalizing polymers, including chitosan, silk fibroin, polyethylene glycol, polyvinyl alcohol, and gelatin, with acrylamide and/or methacrylamide groups.[85,89-92] Although ALMA-based bioinks have been applied in extrusion, inkjet, and microfluidic bioprinting to fabricate spherical, vascular, and microfluidic fiber scaffolds, their application in DLP bioprinting remains limited.[93] Previous studies have demonstrated the feasibility of DLP printing using ALMA-based formulations combined with other photocrosslinkable polymers. For example, ALMA was co-synthesized with GelMA, and hydroxyapatite was incorporated to fabricate high-resolution scaffolds with complex designs. Rapid UV-induced crosslinking produced stable hydrogels with excellent shape fidelity, which were suitable for microporous and macro-channeled bone tissue scaffolds that facilitate cell migration and nutrient transport.[94] Similarly, in pancreatic organoid models, a GelMA/ALMA hydrogel functionalized with the laminin-derived AG73 peptide successfully reproduced native tissue stiffness while maintaining structural integrity throughout long-term culture, owing to the mechanical support of ALMA and the cell-adhesive properties of GelMA. Therefore, the adaptation of ALMA-based hybrid hydrogels for DLP bioprinting represents a promising strategy for combining high-resolution fabrication with the mechanical stability and cytocompatibility required for biomedical applications.[95]

The success of these studies depends not only on material selection but also on the optimization of the underlying bioink formulations and printing parameters. The following section examines these parameters individually, explaining how they affect the printing capability, solubility, and biological performance of ALMA-based DLP bioinks.

5.4. Bioink formulation and printing parameters

3D structures are built by iteratively repeating the photopolymerization process across successive two-dimensional layers, allowing very fine feature resolution.[96] The ability to print ALMA hydrogels with desired properties at high resolution via DLP depends on the type and concentration of the photoinitiator, UV exposure time, and the rheological properties of the ALMA bioink. Therefore, optimizing these parameters is an important consideration for preparing structures with appropriate swelling, degradation, mechanical, and biological performance for the intended application.

5.4.1. Photoinitiators

Photoinitiators play an important role in DLP-based photopolymerization systems. They absorb incident light and convert it into reactive free radicals or ionic species that initiate and propagate chain polymerization throughout the bioink resin.[97] They are divided into two main classes: radical and cationic compounds. For biomedical applications, radical photoinitiators are the standard choice, as cationic systems produce cytotoxic proton species and are therefore largely unsuitable.[98,99]

Radical photoinitiators are further distinguished by their mechanism of radical generation. As illustrated in Figure 8, radical photoinitiators are divided into type I (single-molecule) and type II (two-molecule) systems.[100] Type I systems, which are also known as unimolecular initiators, absorb a photon and undergo rapid, direct homolytic bond cleavage from the excited triplet state, generating two radical fragments that immediately react with methacrylate groups to initiate crosslinking.[99,100] The most widely utilized type I compounds in hydrogel research are 2,2'-azobis[2-methyl-N-(2-hydroxyethyl)propionamide (VA-086), 2-hydroxy-4′-(2-hydroxyethoxy)-2-methylpropiophenone (Irgacure 2959), 2,4,6-trimethylbenzoyl diphenyl phosphine oxide (TPO), germanium-based photoinitiator, and lithium phenyl-2,4,6-trimethylbenzoylphosphinate (LAP). Due to its low cytotoxicity and non-immunogenicity, Irgacure 2959 is used in many UV-cured hydrogels. However, its applicability is limited due to its low solubility. In contrast, LAP is highly soluble in water and can be activated even under visible-light irradiation (405 nm). This photoinitiator enables the fabrication of hydrogel constructs with high cell viability.[98]

Type II systems operate via a fundamentally different bimolecular pathway. Rather than undergoing direct cleavage, the excited initiator reacts with a co-initiator molecule (e.g., a tertiary amine, thiol, or alcohol) by hydrogen abstraction or electron transfer, yielding an active initiating radical on the co-initiator and a non-initiating ketyl radical on the photoinitiator.[100] This bimolecular mechanism is inherently slower and less efficient than type I cleavage. Furthermore, the presence of co-initiators introduces

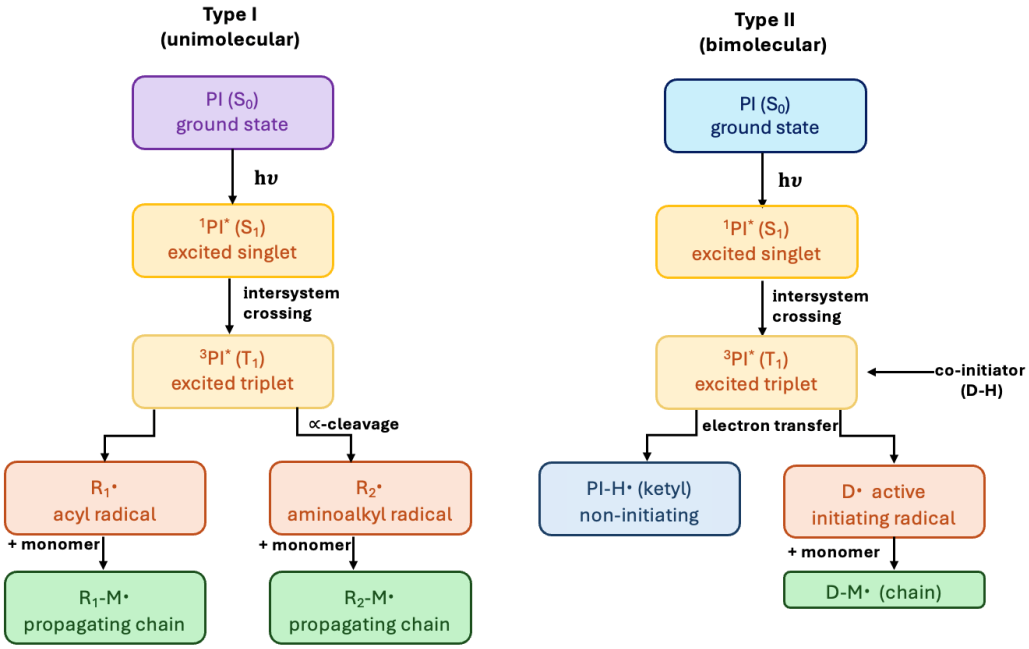


Figure 8. General reaction mechanisms of type I and type II photoinitiators. Type I initiators undergo direct α-cleavage from the excited triplet state (T_1) to generate two reactive radicals (R_1• and R_2•). Type II initiators require a co-initiator (D-H), and the T_1 state abstracts a hydrogen atom or undergoes electron transfer to yield a non-initiating ketyl radical (PI-H•) and an active initiating radical (D•).
Abbreviations: hν: Incident photon energy; S_0: Ground state; S_1: First excited singlet state; T_1: First excited triplet state. Created by the authors using PowerPoint.

additional concerns related to the cytotoxicity and surface migration of unreacted species.[100,101] Nevertheless, type II systems can be designed for activation at visible-light wavelengths, making them more compatible with living cells and applicable to pigmented or optically complex media, in which UV penetration is limited. Riboflavin (vitamin B2), eosin Y (EY), boron dipyrromethene (BODIPY), and tris(2,2-bipyridyl) dichlororuthenium (II) hexahydrate ($Ru(bpy)_3^{2+}$) are representative visible-light photosensitizers used in such systems, all noted for high biocompatibility.[98] Vitamin B2, an endogenous molecule in the body, can initiate polymerization by generating free radicals under blue light (444 nm). Its advantage is high cytocompatibility and low toxicity; however, its slow curing time has prevented widespread use in bioprinting.[102] Eosin Y (EY), while not fast enough alone to generate free radicals for bioprinting, is water-soluble and absorbs green light (515 nm). However, when used with co-initiators such as triethanolamine (TEA), it can provide a faster reaction and higher cell viability. Previous studies have shown that it forms tighter crosslinked networks than UV-activated initiators.[102,103] Similarly, rose bengal activated by green light (520–550 nm) is regarded as a cell-friendly photoinitiator because of its low toxicity and responsiveness to visible-light irradiation.[82] $Ru(bpy)_3Cl_2$ activated at 452 nm visible-light reacts with sodium persulfate (SPS) to generate sulfate radicals that initiate free-radical chain polymerization or thiol-ene photocrosslinking.[82,102] Overall, type II photoinitiators are attractive for bioprinting because of their efficient activation under visible-light irradiation and generally superior biocompatibility compared with conventional UV-activated systems.[82]

To further improve the safety and performance of biomedical DLP bioprinting, photoinitiators with higher initiation efficiency, capable of operating under visible light, lower reactive oxygen species (ROS) production, and lower cytotoxicity, are continuously being developed. Therefore, research efforts have recently focused on the development of novel photoinitiators. Among the currently available systems, LAP, eosin Y, riboflavin (vitamin B2), and $Ru(bpy)_3^{2+}$ are the most widely investigated photoinitiators for bioprinting. In addition, boron dipyrromethene (BODIPY), 2,4,6-trimethylbenzoyl diphenyl phosphine oxide (TPO), and germanium-based photoinitiator derivatives have emerged as promising candidates for future clinical applications.[104-106] BODIPY photoinitiators are activated at low light intensities with a high molar extinction coefficient in a wide wavelength

range of 300–650 nm. Their activation under long-wavelength irradiation rather than UV irradiation makes them promising alternatives for cell-laden hydrogels, as they minimize photodamage to cells and biomolecules.[105] TPO is a highly appropriate photoinitiator for DLP printing, as it offers high quantum efficiency and facilitates rapid polymerization within the 365–405 nm light range.[106] Germanium derivatives have low toxicity and are activated in the 405–450 nm visible-light region. They provide high radical generation efficiency and deep light penetration, thereby improving the resolution and printing efficiency of DLP bioprinting through rapid curing.[104] However, despite their considerable potential, these photoinitiators remain expensive and are still largely confined to laboratory research, requiring further evaluation of long-term cytocompatibility, scalable manufacturing, and regulatory approval before clinical translation. Therefore, selecting an appropriate photoinitiator is a key step in developing ALMA bioinks for DLP applications.

5.4.2. UV exposure time

The UV exposure time is an important parameter in the photopolymerization process of ALMA curing, directly affecting the degree of crosslinking of methacrylate groups and, in turn, the mechanical properties and pore structure.[71] The relationship between light exposure and curing depth is commonly described with Jacobs' curing equation. Jacobs' curing equation is $C_d=D_p \ln(E_0/E_c)$, in which C_d is the cure depth, D_p is the penetration depth, E_0 is the surface exposure energy, and E_c is the critical exposure energy.[107] As the exposure dose is raised, the curing depth also rises until the intended polymer network is achieved. Although the Jacobs' equation estimates curing depth based on exposure energy, it does not predict cell viability. A more comprehensive dose-response model has been proposed for photoactive hydrogels. This model links irradiation wavelength, intensity, and duration to the creation of hydrogel networks and, in turn, cell survival. It offers a flexible basis for predicting cell viability in ALMA-based DLP systems, minimizing the need for extensive testing of every parameter combination.[108]

UV exposure must be carefully optimized because insufficient UV exposure leads to incomplete crosslinking of the network, whereas excessive exposure can cause undesirable results, such as over-hardening, increased brittleness, and cell damage. Experimental evidence has shown this relationship in systems involving photocurable hydrogels. For example, in PVAMA microneedles, extending the exposure duration from 30 s to 50 and then to 70 s led to a gradual enhancement in both the compressive strength and hardness. This change alters the polymer network from a flexible, viscoelastic form to a stiff, glass-like structure that can penetrate the human skin.[109] Similarly, the ALMA hydrogels exhibited an increase in stiffness with extended UV exposure. However, the viability and proliferation of cells progressively decreased with increased irradiation time.[110] In another study, mesenchymal stem cells within a photocrosslinked GelMA hydrogel maintained approximately 75% viability after 4 minutes of irradiation. Viability decreased slightly to approximately 72% after 10 minutes, demonstrating a gradual reduction in cell survival as the exposure time increased.[111] On the other hand, the presence of unreacted substances after polymerization, particularly residual monomers, photoinitiators, and additives, can increase the cytotoxicity of the material. When curing is insufficient, these unreacted harmful monomers and photoinitiators may leak into the surrounding environment, greatly undermining biocompatibility.[112,113] In wells fabricated from PEGDA containing A549 lung epithelial cells, cell viability was influenced by residual unreacted products. This finding underscores the need for extensive curing to improve the cytocompatibility.[112] However, prolonged UV exposure is not ideal because it can directly damage the encapsulated cells.

The UV wavelength also influences the mechanical properties; for example, UV-A (390 nm) light produces a softer and more flexible structure, whereas UV-C (260 nm) light contributes to the formation of a more rigid network.[114] In parallel, it has been reported that bioink formulations containing ALMA and PEGDA can achieve maximum photocrosslinking with gelation times of less than 2 minutes. This result indicates that incorporating a co-crosslinker such as PEGDA can markedly shorten gelation time relative to ALMA alone.[71] These findings indicate that, in ALMA hydrogel systems, UV exposure time and wavelength should be optimized to achieve the desired structural and biological properties.

5.4.3. Rheological properties

In ALMA hydrogel development, the rheological properties of the bioink are important parameters that affect both the physical and biological characteristics of the hydrogel. These properties help determine the viscoelastic behavior and gelation kinetics of the bioink during printing and predict its printability.[77] The viscoelastic characteristics of the material are quantified by storage modulus (G') and the loss modulus (G"), which correspond to solid- and liquid-like behaviors, respectively. When G' is higher than G", the material exhibits the elastic characteristics of the developing structure.[77,115] The point at which the loss and storage moduli intersect is commonly used to identify the sol-gel transition.[77] Identifying this crossover is essential for optimizing the light exposure time required to crosslink hydrogels under UV illumination.[15]

In DLP-based 3D printing, it is important for ALMA bioinks to maintain adequate fluidity at elevated shear rates. An excessively viscous bioink results in an excessively rigid structure, whereas an insufficiently viscous bioink fails to retain its shape after printing. The attainment of shear-thinning characteristics also decreases the mechanical stress imposed on cells during cell printing, thereby aiding in the preservation of cell viability.[15,77] Alginate-based systems exhibit shear-thinning behavior, in which their viscosity decreases as the applied shear rate increases. This attribute enables the bioink to flow smoothly through narrow needles at low pressures.[15,116] In addition to shear-thinning properties, ALMA should exhibit a yield stress to maintain its structural integrity and prevent deformation under the weight of layers applied during printing.[116] However, alginate-based bioinks have some disadvantages, such as low-resolution printing and low viscosity. Owing to their viscous flow behavior, which causes printed structures to spread, alginate solutions alone cannot form stable 3D structures.[117] Although alginate solutions prepared at high concentrations can achieve sufficient viscosity, this characteristic leads to nozzle clogging in extrusion-based 3D printers. To overcome this problem, pre-crosslinking has been applied to low-concentration alginate solutions using ionic crosslinking.[61] This parameter increases the viscosity of the alginate and improves its structural integrity. In addition, a hydrogel microparticle (HMP)-based pre-crosslinking approach has been shown to improve the print quality of ALMA-based inks.[118] Furthermore, blending ALMA with biopolymers such as GelMA, silk fibroin, collagen, and carboxymethylcellulose (CMC) has been reported to improve print quality and structural stability.[77,119,120] Higher concentrations can be used for 3D DLP printing because of the absence of nozzle clogging problems, whereas post-printing settling occurs at lower concentrations. To work at lower concentrations, DS optimization, binary crosslinking strategies, and blending strategies with other biopolymers can be applied to improve structural stability and print quality. Studies on successful 3D DLP printing have not reported standard rheological properties. This is because the printing capability of DLP depends not only on the viscosity and rheological properties, but also on the light duration, penetration, and photoinitiator activity. Reliable printing can be achieved with a relatively low-viscosity formulation with shallow light penetration and high photoinitiator efficiency, similar to a high-viscosity formulation with slow curing kinetics. Therefore, it is not possible to determine the optimum rheological properties of a formulation without considering all the aforementioned parameters.

6. Biomedical applications of ALMA hydrogels

The derivation of ALMA from seaweed offers both lower cost and environmental sustainability advantages compared to many hydrogels, especially in terms of clinical scaling. ALMA hydrogels exhibit an adjustable DS ratio and the ability to regulate features such as swelling, degradation, and mechanical properties to suit the intended application. These materials have been considered for use in several biomedical applications (e.g., wound healing, drug delivery, and tissue engineering). The most important condition for these applications is that the materials are biocompatible. ALMA hydrogel can be produced as a cell-free scaffold, or, depending on the intended application, cells can be added to the ALMA ink before printing to produce hydrogels. Tissue engineering and vascular and neural applications often rely on the production of cell-embedded biomaterials, in which the cells are homogeneously distributed in the bioink and photoencapsulated during DLP printing. For drug delivery and wound healing applications, ALMA is printed in a cell-free manner. Biological activity is derived from either the encapsulated therapeutic agent or the host tissue, rather than from the printed cells.

6.1. Tissue engineering

ALMA provides multidimensional contributions to tissue engineering as a 3D scaffold material. By conjugating RGD peptides, heparin analogs, or cell-binding ligands to ALMA chains, the materials can be transformed into biointeractive structures that support cell proliferation and differentiation. Tissue engineering enables the production of cell-loaded 3D biomaterials that closely replicate native tissue architecture and environment.[121] For tissue engineering applications, cells are homogeneously dispersed into ALMA ink prepared in the dark to form the hydrogel. These biocompatible systems have been used to create 3D models of several organs, including the heart, kidneys, lungs, nerves, muscles, cartilage, skin, and liver. Compared with two-dimensional systems, these structures possess superior geometry and exhibit biomimetic behavior that more closely matches that of living tissues.[121,122]

ALMA functions as a biomimetic ECM-like material that supports cell adhesion, proliferation, and differentiation. Its mechanical versatility makes it suitable for a range of applications, from soft to hard tissues.[14] Photocrosslinked alginate hydrogels exhibit mechanical properties up to seven times those of their ionically crosslinked counterparts, while more faithfully replicating ECM-like microenvironments.[11] Dual-crosslinked AEMA-modified alginate microbeads have demonstrated significantly

enhanced *in vivo* stability, maintaining structural integrity for three weeks in rat implantation models, whereas unmodified alginate constructs deteriorated within the first week.[60] However, photocrosslinked alginate hydrogels degrade more slowly *in vivo* than *in vitro*, which may limit certain applications.[123]

The self-healing limitations associated with the avascular nature of cartilage make ALMA-based hydrogels an attractive option for cartilage repair.[124] ALMA can be tuned to balance stiffness and elasticity, producing scaffolds that withstand cyclic loading in a joint environment.[59]

6.2. Vascular and neural applications

The integration of ALMA with microfluidic platforms and 3D bioprinting provides opportunities for *in vitro* modeling of vascular channels and complex neural networks. In vascular tissue engineering, ALMA microfibers fabricated using coaxial pressure nozzles create permeable microchannels. These microchannels enable the transport of oxygen and nutrients to the tissues.[49,67] ALMA hydrogels are considered biomaterials that support neural cell adhesion and orientation because of their tunable mechanical features and capability to be produced at the microscale with high resolution. Optimizing the surface and structural properties of ALMA hydrogels can improve neural cell interactions and facilitate the use of the materials for nerve tissue engineering applications.[59]

6.3. Drug delivery

UV curable and covalently bonded 3D ALMA hydrogels can be modified to provide controlled release functionality for drug delivery applications. For example, the drug release properties of doxorubicin-loaded ALMA hydrogels and dual crosslinked ALMA hydrogels with $CaCl_2$ have been investigated. Single ALMA hydrogels loaded with a higher amount of drugs were associated with a faster release; in contrast, double-crosslinked ALMA hydrogels loaded with fewer drugs were associated with slower release kinetics.[125] This finding suggests that the drug release properties of ALMA can be modified to suit the targeted treatment by adjusting crosslinking density. In another study, doxorubicin-loaded ALMA hydrogels were evaluated in a cancer-mimicking microenvironment; the release of 85% of the encapsulated drug over six days was reported [73]. ALMA hydrogels can adapt to and respond to stimuli in biological media. For orally administered medications that need protection from the gastric environment, ALMA hydrogels are noted to constrict in the gastric environment to protect the drug during delivery to the intestine and then expand again at intestinal pH to enable the release of the drug.[126]

6.4. Wound healing

ALMA hydrogels maintain a moist wound environment, facilitating cell adhesion and promoting tissue regeneration during wound healing. Additionally, these hydrogels enable the controlled release of medications at the wound region and can be employed alongside antibacterial agents to mitigate the risk of infection.[127,128] Furthermore, ALMA can be used effectively for sutureless wound closure. For this purpose, a mixture of ALMA and a photoinitiator liquid solution, prepared in a dark environment, rapidly forms a gel when injected into the wound under appropriate conditions and exposed to UV light. The use of ALMA in combination with an argon laser can shorten surgery time and reduce the risk of complications. Additionally, ALMA hydrogels exhibit over 80% light transmittance, allowing for the noninvasive monitoring of wound healing, thus preserving the integrity of the newly formed tissue.[76]

7. Current challenges and future perspectives

Efforts involving ALMA-based DLP bioinks are currently focused on the optimization phase of bioink formulation and printing parameters. These laboratory-scale studies must be reproducible and clinically validated before large-scale production. The sensitivity of ALMA bioinks to processing conditions poses a significant challenge. Variations in alginate type, methacrylation method, DS, photoinitiator type, and light exposure can affect the printing capability and final mechanical and biological properties of the structure. Therefore, the standardization of material preparation and printing conditions is important to improve repeatability. To overcome these challenges, predictive systems such as artificial intelligence (AI) and machine learning (ML) have begun to replace trial-and-error approaches. In the design phase of materials, such as artificial organs and tissues, ML can predict structural performance under different conditions by optimizing material geometry. In addition, mechanically enhanced structures are printed by saving material through the optimization of design geometry.[129] For example, in a DLP-based 3D printer working with the vat polymerization principle, the problem of pixel-induced jagged edges during printing is minimized by applying hybrid ML.[82,130] In the realm of bioprinting, AI enhances the quality of prints by optimizing the process, enabling real-time monitoring, and employing predictive modeling to increase efficiency[129] and the print time is shortened without compromising quality.[82] While the limited interpretability of many ML models remains a challenge for clinical translation, AI-driven approaches are becoming important for developing autonomous, efficient,

and reliable bioprinting systems.[129] The application of these predictive strategies to DLP formulations that utilize ALMA requires further exploration in future studies. Beyond advances in AI, standardization is equally important for comparing the results of different studies and facilitating their translation into clinical practice. Future studies should develop standardized protocols for material characterization, printing performance, mechanical testing, cytocompatibility, and reproducibility in accordance with ASTM and ISO guidelines. In 2024, the ASTM published bioink guidelines offering recommendations for cell-based or cell-free bioinks.[131] However, these guidelines address only extrusion-based bioprinting, and an equivalent standard specifically covering vat photopolymerization processes has not yet been established. In addition to technical standardization, regulatory considerations are a significant challenge. From a regulatory perspective, photocurable bioinks are evaluated as part of the final medical device rather than as stand-alone biomaterials. To date, no photocrosslinkable bioink, including ALMA, has received FDA approval for cell-laden applications in the biomedical field.[132,133] Instead, the FDA assesses the safety and performance of the completed device in its intended clinical application.[81,133] Although photocurable resins have been approved for applications such as dental devices and surgical guides, no comparable regulatory pathway currently exists for soft cell-encapsulating bioinks. As such, advancing ALMA-based bioinks for preclinical and clinical use will require comprehensive quality assurance throughout the entire manufacturing workflow, including alginate extraction, chemical modification, sterilization, photo-curing, and post-printing biological evaluation.

8. Conclusions

The fabrication of ALMA hydrogels via DLP involves three distinct stages: seaweed-based alginate extraction, methacrylation, and light-driven 3D printing, each introducing variables that influence the properties of the final product. The molecular weight, viscosity, and the M/G ratio of alginate are not inherent constants of the material; they result from various biological and processing choices, such as brown seaweed species, location, harvest season, and the extraction technique used. These variables affect the methacrylation efficiency and, ultimately, the mechanical and degradation properties of the 3D DLP-printed ALMA hydrogel. Methacrylation with different agents provides researchers with meaningful control over crosslink density, swelling, and stiffness. DLP printing enhances the capabilities of ALMA systems. Its ability to achieve high spatial resolution and *in situ* curing is challenging to replicate using extrusion or ionic gelation techniques. However, even minor changes in the rheological properties of the bioink or photoinitiator concentration can compromise layer adhesion or introduce cytotoxic residues. Previous studies have confirmed the utility of individual bioink components without rigorously examining their interactions. Addressing this gap is a critical priority for future research on the 3D DLP fabrication of ALMA hydrogels. Establishing protocols that carefully monitor a single batch from the initial extraction of alginate through methacrylation to the final DLP printing output, while assessing the impact of each procedural step, will considerably improve bioink design. From a biological perspective, the differences between the *in vitro* and *in vivo* degradation rates of photocrosslinked ALMA remain poorly understood, limiting the reliable translation of scaffold designs to animal and clinical models. Future efforts in this area will involve treating extraction, methacrylation, and DLP fabrication as a cohesive process, in which each choice is linked to a biological or mechanical outcome rather than as separate stages.

Acknowledgments

None.

Funding

This work was supported by the Scientific and Technological Research Council of Türkiye (TÜBİTAK) under Project No. 224M659.

Conflict of interest

The authors declare they have no competing interests.

Author contributions

Conceptualization: Merve Ilgar, Oguzhan Gunduz, Roger Narayan

Visualization: Merve Ilgar, Eylul Dila Carkci, Elif Emekdar

Writing–original draft: Merve Ilgar, Eylul Dila Carkci, Elif Emekdar

Writing–review & editing: Oguzhan Gunduz, Roger Narayan

Ethics approval and consent to participate

Not applicable.

Consent for publication

Not applicable.

Availability of data

Not applicable.

Further disclosure

AI-assisted language editing tools (Paperpal) were used

to improve the grammatical accuracy of this review. Illustrations were created using BioRender (BioRender.com). The authors take full responsibility for the integrity and accuracy of the scientific content presented.

References

1. Bi D, Yang X, Yao L, *et al*. Potential Food and Nutraceutical Applications of Alginate: A Review. *Marine Drugs*. 2022;20(9):564.

   doi: 10.3390/md20090564

2. Wang Y, Lu Y. Sodium Alginate-Based Functional Materials toward Sustainable Applications: Water Treatment and Energy Storage. *Ind Eng Chem Res*. 2023;62(29):11279-11304.

   doi: 10.1021/acs.iecr.3c01082

3. Jain D, Bar-Shalom D. Alginate drug delivery systems: Application in context of pharmaceutical and biomedical research. *Drug Dev Ind Pharm*. 2014;40(12):1576-1584.

   doi: 10.3109/03639045.2014.917657

4. Farshidfar N, Iravani S, Varma RS. Alginate-Based Biomaterials in Tissue Engineering and Regenerative Medicine. *Marine Drugs*. 2023;21(3):189.

   doi: 10.3390/md21030189

5. Li Y, Liao J, Li S, *et al*. Marine materials: New hope for biomedical applications. *Cell Biomaterials*. 2026;2(8):100370.

   doi: 10.1016/j.celbio.2026.100370

6. Fernando IPS, Lee WW, Han EJ, Ahn G. Alginate-based nanomaterials: Fabrication techniques, properties, and applications. *Chem Eng J*. 2020;391(4472):123823.

   doi: 10.1016/j.cej.2019.123823

7. Peteiro C. Alginate Production from Marine Macroalgae, with Emphasis on Kelp Farming. In: *Springer Series in Biomaterials Science and Engineering*. Singapore: Springer; 2017:27-66.

   doi: 10.1007/978-981-10-6910-9_2

8. Saji S, Hebden A, Goswami P, Du C. A Brief Review on the Development of Alginate Extraction Process and Its Sustainability. *Sustainability*. 2022;14(9):5181.

   doi: 10.3390/su14095181

9. Bojorges H, López-Rubio A, Martínez-Abad A, Fabra J. Overview of alginate extraction processes: Impact on alginate molecular structure and techno-functional properties. *Trends Food Sci Technol*. 2023;140:104142.

   doi: 10.1016/j.tifs.2023.104142

10. Fawzy MA, Gomaa M, Hifney AF, Abdel-Gawad KM. Optimization of alginate alkaline extraction technology from Sargassum latifolium and its potential antioxidant and emulsifying properties. *Carbohydr Polym*. 2017;157:1903-1912.

    doi: 10.1016/J.CARBPOL.2016.11.077

11. Stagnaro P, Schizzi I, Utzeri R, Marsano E, Castellano M. Alginate-polymethacrylate hybrid hydrogels for potential osteochondral tissue regeneration. *Carbohydr Polym*. 2018;185:56-62.

    doi: 10.1016/j.carbpol.2018.01.012

12. Chou AI, Nicoll SB. Characterization of photocrosslinked alginate hydrogels for nucleus pulposus cell encapsulation. *J Biomed Mater Res A*. 2009;91A(1):187-194.

    doi: 10.1002/jbm.a.32191

13. Wang X, Hao T, Qu J, Wang C, Chen H. Synthesis of Thermal Polymerizable Alginate-GMA Hydrogel for Cell Encapsulation. *J Nanomater*. 2015;2015(1): 970619.

    doi: 10.1155/2015/970619

14. Araiza-Verduzco F, Rodríguez-Velázquez E, Cruz H, *et al*. Photocrosslinked Alginate-Methacrylate Hydrogels with Modulable Mechanical Properties: Effect of the Molecular Conformation and Electron Density of the Methacrylate Reactive Group. *Materials*. 2020;13(3):534.

    doi: 10.3390/ma13030534

15. Mishbak HH, Cooper G, Bartolo PJ. Development and characterization of a photocurable alginate bioink for three-dimensional bioprinting. *Int J Bioprint*. 2019;5(2):189.

    doi: 10.18063/ijb.v5i2.189

16. Flórez-Fernández N, Domínguez H, Torres MD. A green approach for alginate extraction from Sargassum muticum brown seaweed using ultrasound-assisted technique. *Int J Biol Macromol*. 2019;124:451-459.

    doi: 10.1016/j.ijbiomac.2018.11.232

17. Makoure D, Arhaliass A, Echchelh A, Baron R, Legrand J. Procédé d'extrusion réactive et/ou enzymatique pour l'extraction de phycocolloïdes: application aux produits de la mer [Reactive and/or enzymatic extrusion process for phycocolloids extraction: application to sea products]. *STA*. 2019;2(1). [In French]

    doi: 10.21494/iste.op.2021.0675

18. Nesic A, De Bonis MV, Dal Poggetto G, Ruocco G, Santagata G. Microwave Assisted Extraction of Raw Alginate as a Sustainable and Cost-Effective Method to Treat Beach-Accumulated Sargassum Algae. *Polymers*. 2023;15(14).

    doi: 10.3390/polym15142979

19. Ummat V, Zhao M, Sivagnanam SP, *et al*. Ultrasound-Assisted Extraction of Alginate from Fucus vesiculosus Seaweed By-Product Post-Fucoidan Extraction. *Marine Drugs*. 2024;22(11).

    doi: 10.3390/md22110516

20. Ye S, Xie C, Agar OT, Barrow CJ, Dunshea FR, Suleria HAR.

Alginates from Brown Seaweeds as a Promising Natural Source: A Review of Its Properties and Health Benefits. *Food Reviews International*. 2024;40(9):2682-2710.

doi: 10.1080/87559129.2023.2279583

21. Trica B, Delattre C, Gros F, *et al*. Extraction and Characterization of Alginate from an Edible Brown Seaweed (Cystoseira barbata) Harvested in the Romanian Black Sea. *Marine Drugs*. 2019;17(7).

doi: 10.3390/md17070405

22. Nøkling-Eide K, Langeng AM, Åslund A, Aachmann FL, Sletta H, Arlov Ø. An assessment of physical and chemical conditions in alginate extraction from two cultivated brown algal species in Norway: Alaria esculenta and Saccharina latissima. *Algal Res*. 2023;69(1-2):102951.

doi: 10.1016/j.algal.2022.102951

23. Wedlock DJ, Fasihuddin BA. Effect of formaldehyde pre-treatment on the intrinsic viscosity of alginate from various brown seaweeds. *Food Hydrocoll*. 1990;4(1):41-47.

doi: 10.1016/S0268-005X(09)80326-3

24. Shi Y, Dong M, Lei X, *et al*. Comparison of Flocculation Methods for Sodium Alginate and Characterization of Its Structure and Properties. Published online 2025.

doi: 10.3390/foods14172970

25. Qin Y. The Extraction of Alginate from Brown Seaweeds. In: *Alginate Fibers and Wound Dressings*. Hoboken, NJ: Wiley; 2023.

doi: 10.1002/9783527845200.ch1

26. Mohammed A, Bissoon R, Bajnath E, *et al*. Multistage extraction and purification of waste Sargassum natans to produce sodium alginate: An optimization approach. *Carbohydr Polym*. 2018;198:109-118.

doi: 10.1016/J.CARBPOL.2018.06.067

27. Vauchel P, Kaas R, Arhaliass A, Baron R, Legrand J. A New Process for Extracting Alginates from Laminaria digitata: Reactive Extrusion. *Food Bioprocess Technol*. 2008;1(3):297-300.

doi: 10.1007/s11947-008-0082-x

28. Baron R, Vauchel P, Kaas R, Arhaliass A, Legrand J. Dynamical modelling of a reactive extrusion process: Focus on residence time distribution in a fully intermeshing co-rotating twin-screw extruder and application to an alginate extraction process. *Chem Eng Sci*. 2010;65(10):3313-3321.

doi: 10.1016/j.ces.2010.02.019

29. Baron R, Vauchel P, Arhaliass A. Modeling of twin-screw reactive extrusion: application to alginate extraction. *IFAC Proceedings Volumes*. 2010;43(6):341-346.

doi: 10.3182/20100707-3-BE-2012.0094

30. Felicia WXL, Rovina K, Zuldin WH, Suriati L, Huda N, Nurdiani R. Sustainable Valorization of Alginate, a Review of Green Extraction, Structure–Function Relationships, and Next-Generation Food Applications. *Food and Bioprocess Technology*. 2026;19(2):97.

doi: 10.1007/S11947-025-04096-X

31. Savić Gajić IM, Savić IM, Ivanovska AM, Vunduk JD, Mihalj IS, Svirčev ZB. Improvement of Alginate Extraction from Brown Seaweed (Laminaria digitata L.) and Valorization of Its Remaining Ethanolic Fraction. *Marine Drugs*. 2024;22(6).

doi: 10.3390/MD22060280

32. Youssouf L, Lallemand L, Giraud P, *et al*. Ultrasound-assisted extraction and structural characterization by NMR of alginates and carrageenans from seaweeds. *Carbohydr Polym*. 2017;166:55-63.

doi: 10.1016/J.CARBPOL.2017.01.041

33. Dodero A, Vicini S, Castellano M. Depolymerization of sodium alginate in saline solutions via ultrasonic treatments: A rheological characterization. *Food Hydrocoll*. 2020;109:106128.

doi: 10.1016/J.FOODHYD.2020.106128

34. Yuan Y, Macquarrie D. Microwave assisted extraction of sulfated polysaccharides (fucoidan) from Ascophyllum nodosum and its antioxidant activity. *Carbohydr Polym*. 2015;129(10):101-107.

doi: 10.1016/j.carbpol.2015.04.057

35. Abdul Khalil HPS, Lai TK, Tye YY, *et al*. A review of extractions of seaweed hydrocolloids: Properties and applications. *Express Polym Lett*. 2018;12(4):296-317.

doi: 10.3144/expresspolymlett.2018.27

36. Nam H Bin, Lee KH, Yoo HY, Park C, Lim JM, Lee JH. Rapid and High-Yield Recovery of Sodium Alginate from Undaria pinnatifida via Microwave-Assisted Extraction. *Processes*. 2024;12(1).

doi: 10.3390/pr12010208

37. Sugiono S, Hidayat MT, Alrosyidi F, *et al*. Microwave-Assisted Extraction in A Sequential Biorefinery of Alginate and Fucoidan From Brown Alga Sargassum Cristaefolium. *Food Sci Technol*. Published online December 1, 2022:96-105.

doi: 10.25139/fst.vi.4976

38. Andriamanantoanina H, Rinaudo M. Characterization of the alginates from five madagascan brown algae. *Carbohydr Polym*. 2010;82(3):555-560.

doi: 10.1016/j.carbpol.2010.05.002

39. Sari-Chmayssem N, Taha S, Mawlawi H, Guégan JP, Jeftić J, Benvegnu T. Extracted and depolymerized alginates from brown algae Sargassum vulgare of Lebanese origin: chemical, rheological, and antioxidant properties. *J Appl*

Phycol. 2016;28(3):1915-1929.

doi: 10.1007/s10811-015-0676-4

40. Khajouei RA, Keramat J, Hamdami N, *et al*. Extraction and characterization of an alginate from the Iranian brown seaweed Nizimuddinia zanardini. *Int J Biol Macromol*. 2018;118:1073-1081.

doi: 10.1016/j.ijbiomac.2018.06.154

41. Sugiono S, Masruri M, Estiasih T, Widjanarko SB. Optimization of extrusion-assisted extraction parameters and characterization of alginate from brown algae (Sargassum cristaefolium). *J Food Sci Technol.* 2019;56(8):3687-3696.

doi: 10.1007/S13197-019-03829-Z

42. Mohammed A, Rivers A, Stuckey DC, Ward K. Alginate extraction from Sargassum seaweed in the Caribbean region: Optimization using response surface methodology. *Carbohydr Polym*. 2020;245:116419.

doi: 10.1016/J.CARBPOL.2020.116419

43. Chica LR, Yamashita C, Nunes NSS, *et al*. Optimizing alginate extraction using Box-Behnken design: Improving yield and antioxidant properties through ultrasound-assisted citric acid extraction. *Food Chem Adv*. 2024;5:100813.

doi: 10.1016/J.FOCHA.2024.100813

44. Smith HA, Cabling LPB, Leonard NA, Dubrawski KL, Buckley HL. Green Alginate Extraction from Macrocystis pyrifera for Bioplastic Applications: Physicochemical, Environmental Impact, and Chemical Hazard Analyses. *ACS Sustain Resour Manag*. 2024;1(5):958-969.

doi: 10.1021/acssusresmgt.4c00019

45. Alboofetileh M, Jeddi S, Abdollahi M. Sequential recovery of alginate from fucoidan extraction by-products of Nizamuddinia zanardinii seaweed using green extraction methods. *Ultrason Sonochem*. 2025;117:107343.

doi: 10.1016/J.ULTSONCH.2025.107343

46. Varaprasad K, Jayaramudu T, Kanikireddy V, Toro C, Sadiku ER. Alginate-based composite materials for wound dressing application:A mini review. *Carbohydr Polym*. 2020;236:116025.

doi: 10.1016/j.carbpol.2020.116025

47. Jiao W, Chen W, Mei Y, *et al*. Effects of Molecular Weight and Guluronic Acid/Mannuronic Acid Ratio on the Rheological Behavior and Stabilizing Property of Sodium Alginate. *Molecules*. 2019;24(23).

doi: 10.3390/molecules24234374

48. Hernández-González AC, Téllez-Jurado L, Rodríguez-Lorenzo LM. Alginate hydrogels for bone tissue engineering, from injectables to bioprinting: A review. *Carbohydr Polym*. 2020;229:115514.

doi: 10.1016/J.CARBPOL.2019.115514

49. Axpe E, Oyen M. Applications of Alginate-Based Bioinks in 3D Bioprinting. *Int J Mol Sci*. 2016;17(12):1976.

doi: 10.3390/ijms17121976

50. Ching SH, Bansal N, Bhandari B. Alginate gel particles–A review of production techniques and physical properties. *Crit Rev Food Sci Nutr*. 2017;57(6):1133-1152.

doi: 10.1080/10408398.2014.965773

51. Liu J, Yang S, Li X, Yan Q, Reaney MJT, Jiang Z. Alginate Oligosaccharides: Production, Biological Activities, and Potential Applications. *Compr Rev Food Sci Food Saf*. 2019;18(6):1859-1881.

doi: 10.1111/1541-4337.12494

52. Hariyadi DM, Islam N. Current Status of Alginate in Drug Delivery. *Adv Pharmacol Pharm Sci*. 2020;2020:1-16.

doi: 10.1155/2020/8886095

53. Cardoso M, Costa R, Mano J. Marine Origin Polysaccharides in Drug Delivery Systems. *Mar Drugs*. 2016;14(2):34.

doi: 10.3390/md14020034

54. Deng Y, Shavandi A, Okoro OV, Nie L. Alginate modification via click chemistry for biomedical applications. *Carbohydr Polym*. 2021;270:118360.

doi: 10.1016/j.carbpol.2021.118360

55. Kumar B, Singh N, Kumar P. A review on sources, modification techniques, properties and potential applications of alginate-based modified polymers. *Eur Polym J*. 2024;213:113078.

doi: 10.1016/J.EURPOLYMJ.2024.113078

56. Jeon O, Bouhadir KH, Mansour JM, Alsberg E. Photocrosslinked alginate hydrogels with tunable biodegradation rates and mechanical properties. *Biomaterials*. 2009;30(14):2724-2734.

doi: 10.1016/J.BIOMATERIALS.2009.01.034

57. Wang H, Bu X, Huang Z, Yang J, Qiu T. Synthesis of Methacrylic Anhydride by Batch Reactive Distillation: Reaction Kinetics and Process. *Ind Eng Chem Res*. 2014;53(44):17317-17324.

doi: 10.1021/IE501607V

58. Habib M, Berthalon S, Leclercq L, Tourrette A, Sharkawi T, Blanquer S. Dual Cross-Linked Stimuli-Responsive Alginate-Based Hydrogels. *Biomacromolecules*. 2024;25(3):1660-1670.

doi: 10.1021/ACS.BIOMAC.3C01201

59. Hasany M, Talebian S, Sadat S, *et al*. Synthesis, properties, and biomedical applications of alginate methacrylate (ALMA)-based hydrogels: Current advances and challenges. *Appl Mater Today*. 2021;24:101150.

doi: 10.1016/j.apmt.2021.101150

60. Somo SI, Langert K, Yang CY, *et al*. Synthesis and evaluation of dual crosslinked alginate microbeads. *Acta Biomater*. 2018;65:53-65.

doi: 10.1016/J.ACTBIO.2017.10.046

61. Liang X, Chen S, Liang Y, *et al*. Alginate-Based Hydrogels: Recent Progress in Preparation, Property Tuning, and Multifunctional Applications. *Gels*. 2026;12(2):182.

doi: 10.3390/gels12020182

62. Ren Y, Wang Q, Xu W, *et al*. Alginate-based hydrogels mediated biomedical applications: A review. *Int J Biol Macromol*. 2024;279:135019.

doi: 10.1016/J.IJBIOMAC.2024.135019

63. Tansik G, Stowers R. Viscoelastic and phototunable GelMA-alginate hydrogels for 3D cell culture. *MRS Advances*. 2024;9(8):505-511.

doi: 10.1557/S43580-024-00815-2

64. Tavafoghi M, Sheikhi A, Tutar R, *et al*. Engineering tough, injectable, naturally-derived, bioadhesive composite hydrogels. *Adv Healthc Mater*. 2020;9(10):e1901722.

doi: 10.1002/ADHM.201901722

65. Yue H, Wang Y, Fernandes S, Vyas C, Bartolo P. Bioprinting of GelMA/PEGDA Hybrid Bioinks for SH-SY5Y Cell Encapsulation: Role of Molecular Weight and Concentration. *Macromol Biosci*. 2025;25(6).

doi: 10.1002/MABI.202400587

66. Yang W, Liu R, Qian K, *et al*. 3D-printed cell-free bioactive scaffolds from methacrylated hyaluronic acid and silk fibroin incorporating platelet-rich plasma for adipose tissue regeneration. *Int J Biol Macromol*. 2026;365:152341.

doi: 10.1016/j.ijbiomac.2026.152341

67. Gao Y, Jin X. Dual Crosslinked Methacrylated Alginate Hydrogel Micron Fibers and Tissue Constructs for Cell Biology. *Mar Drugs*. 2019;17(10):557.

doi: 10.3390/MD17100557

68. García-García A, Silván U, Pérez-Álvarez L, Lanceros S. Comparing the Printability, Biological and Physicochemical Properties of Bio-Based Photo-Crosslinkable Hydrogels. *Polymers*. 2025;17(21):2867.

doi: 10.3390/POLYM17212867

69. Augst AD, Kong HJ, Mooney DJ. Alginate hydrogels as biomaterials. *Macromol Biosci*. 2006;6(8):623-633.

doi: 10.1002/MABI.200600069

70. Masoumi Shahrbabak S, Jalali SM, Fathabadi MF, *et al*. Modified alginates for precision drug delivery: Advances in controlled-release and targeting systems. *Int J Pharm X*. 2025;10:100381.

doi: 10.1016/J.IJPX.2025.100381

71. Zoco de la Fuente A, García-García A, Pérez-Álvarez L, *et al*. Evaluation of Various Types of Alginate Inks for Light-Mediated Extrusion 3D Printing. *Polymers*. 2024;16(7):986.

doi: 10.3390/POLYM16070986

72. Chou AI, Akintoye SO, Nicoll SB. Photo-crosslinked alginate hydrogels support enhanced matrix accumulation by nucleus pulposus cells in vivo. *Osteoarthritis Cartilage*. 2009;17(10):1377-1384.

doi: 10.1016/j.joca.2009.04.012

73. Batool SR, Nazeer MA, Ekinci D, Sahin A, Kizilel S. Multifunctional alginate-based hydrogel with reversible crosslinking for controlled therapeutics delivery. *Int J Biol Macromol*. 2020;150:315-325.

doi: 10.1016/J.IJBIOMAC.2020.02.042

74. Tahir I, Floreani R. Dual-Crosslinked Alginate-Based Hydrogels with Tunable Mechanical Properties for Cultured Meat. *Foods*. 2022;11(18).

doi: 10.3390/foods11182829

75. Jalali Kandeloos A, Bastani S, Mashayekhan S. Architecting oxidized alginate methacrylate hydrogels with tunable characteristics by altering the sequence of the cross-linking steps, methacrylation reaction time, and polymer concentration. *J Biomater Appl*. 2023;38(1):25-38.

doi: 10.1177/08853282231184294

76. Mignon A, Zimmer J, Gutierrez Cisneros C, *et al*. Electron-Beam-Initiated Crosslinking of Methacrylated Alginate and Diacrylated Poly(ethylene glycol) Hydrogels. *Polymers (Basel)*. 2023;15(24):4685.

doi: 10.3390/POLYM15244685

77. Lipari S, Sacco P, Marsich E, Donati I. Silk Fibroin-Enriched Bioink Promotes Cell Proliferation in 3D-Bioprinted Constructs. Published online 2024.

doi: 10.3390/gels10070469

78. Poshina D, Sokolova N, Nono-Tagne S, *et al*. Electrospinning of methacrylated alginate for tissue engineering applications. *RSC Adv*. 2024;14(52):38746-38756.

doi: 10.1039/D4RA07559E

79. Gutierrez Cisneros C, Agten H, Derveaux E, Adriaensens P, Bloemen V, Mignon A. Development of a biocompatible, low-cost reinforcement of methacrylated alginate hydrogels using synthetic crosslinking agents. *React Funct Polym*. 2025;214:106330.

doi: 10.1016/J.REACTFUNCTPOLYM.2025.106330

80. International Organization for Standardization. *Additive manufacturing — General principles — Fundamentals and vocabulary.* ISO/ASTM 52900:2021. Accessed July 26, 2026. https://www.iso.org/standard/74514.html

81. Ng WL, An J, Chua CK. Process, Material, and Regulatory

Considerations for 3D Printed Medical Devices and Tissue Constructs. *Engineering*. 2024;36:146-166.

doi: 10.1016/J.ENG.2024.01.028

82. Ng WL, Paula CTB, Serra AC, Coelho JFJ, Bartolo P. Vat photopolymerization-based bioprinting: Shaping next-generation tissues with light. *Interd Med*. 2026;4(1):e70078.

doi: 10.1002/INMD.70078

83. Li Y, Zhang X, Zhang X, Zhang Y, Hou D. Recent Progress of the Vat Photopolymerization Technique in Tissue Engineering: A Brief Review of Mechanisms, Methods, Materials, and Applications. *Polymers*. 2023;15(19):3940.

doi: 10.3390/POLYM15193940

84. Islam A, Rahman MZ. Recent advances in additive manufacturing techniques: An in-depth review. *Comprehensive Materials Processing: Volume 1-13, Second edition*. 2024;13:352-378.

doi: 10.1016/B978-0-323-96020-5.00187-4

85. Li H, Dai J, Wang Z, *et al*. Digital light processing (DLP)-based (bio)printing strategies for tissue modeling and regeneration. *Aggregate*. 2023;4(2).

doi: 10.1002/agt2.270

86. Zhao T, Liu Y, Wu Y, Zhao M, Zhao Y. Controllable and biocompatible 3D bioprinting technology for microorganisms: Fundamental, environmental applications and challenges. *Biotechnol Adv*. 2023;69:108243.

doi: 10.1016/j.biotechadv.2023.108243

87. Kowsari K, Zhang B, Panjwani S, *et al*. Photopolymer formulation to minimize feature size, surface roughness, and stair-stepping in digital light processing-based three-dimensional printing. *Addit Manuf*. 2018;24:627-638.

doi: 10.1016/j.addma.2018.10.037

88. Bhusal A, Dogan E, Nguyen HA, *et al*. Multi-material digital light processing bioprinting of hydrogel-based microfluidic chips. *Biofabrication*. 2022;14(1):014103.

doi: 10.1088/1758-5090/ac2d78

89. Goodarzi Hosseinabadi H, Nieto D, Yousefinejad A, Fattel H, Ionov L, Miri AK. Ink material selection and optical design considerations in DLP 3D printing. *Appl Mater Today*. 2023;30:101721.

doi: 10.1016/j.apmt.2022.101721

90. Grigoryan B, Paulsen SJ, Corbett DC, *et al*. Multivascular networks and functional intravascular topologies within biocompatible hydrogels. *Science*. 2019;364(6439):458-464.

doi: 10.1126/science.aav9750

91. He Y, Wang F, Wang X, Zhang J, Wang D, Huang X. A photocurable hybrid chitosan/acrylamide bioink for DLP based 3D bioprinting. *Mater Des*. 2021;202:109588.

doi: 10.1016/j.matdes.2021.109588

92. Na K, Shin S, Lee H, *et al*. Effect of solution viscosity on retardation of cell sedimentation in DLP 3D printing of gelatin methacrylate/silk fibroin bioink. *J Ind Eng Chem*. 2018;61:340-347.

doi: 10.1016/j.jiec.2017.12.032

93. Piras CC, Smith DK. Multicomponent polysaccharide alginate-based bioinks. *J Mater Chem B*. 2020;8(36):8171-8188.

doi: 10.1039/D0TB01005G

94. Ren X, Wang J, Wu Y, *et al*. One-pot synthesis of hydroxyapatite hybrid bioinks for digital light processing 3D printing in bone regeneration. *J Mater Sci Technol*. 2024;188:84-97.

doi: 10.1016/J.JMST.2024.01.001

95. Wan J, Xu Y, Qi T, *et al*. AG73-GelMA/AlgMA hydrogels provide a stable microenvironment for the generation of pancreatic progenitor organoids. *J Nanobiotechnol*. 2025;23(1):149.

doi: 10.1186/S12951-025-03266-5

96. Li Y, Mao Q, Yin J, Wang Y, Fu J, Huang Y. Theoretical prediction and experimental validation of the digital light processing (DLP) working curve for photocurable materials. *Addit Manuf*. 2021;37:101716.

doi: 10.1016/j.addma.2020.101716

97. Allen NS. Photoinitiators for UV and visible curing of coatings: Mechanisms and properties. *J Photochem Photobiol A Chem*. 1996;100(1-3):101-107.

doi: 10.1016/S1010-6030(96)04426-7

98. Tomal W, Ortyl J. Water-Soluble Photoinitiators in Biomedical Applications. *Polymers*. 2020;12(5):1073.

doi: 10.3390/POLYM12051073

99. Wang Y, Zhang S, Wang J. Photo-crosslinkable hydrogel and its biological applications. *Chin Chem Lett*. 2021;32(5):1603-1614.

doi: 10.1016/j.cclet.2020.11.073

100. Yagci Y, Jockusch S, Turro NJ. Photoinitiated Polymerization: Advances, Challenges, and Opportunities. *Macromolecules*. 2010;43(15):6245-6260.

doi: 10.1021/MA1007545

101. Dzwonkowska-Zarzycka M, Sionkowska A. Photoinitiators for Medical Applications—The Latest Advances. *Molecules*. 2024;29(16):3898.

doi: 10.3390/MOLECULES29163898

102. Elkhoury K, Zuazola J, Vijayavenkataraman S. Bioprinting the future using light: A review on photocrosslinking reactions, photoreactive groups, and photoinitiators. *SLAS Technol*. 2023;28(3):142-151.

doi: 10.1016/J.SLAST.2023.02.003

103. Kim M, Kang D, Han H, Jang J. Light-activated decellularized extracellular matrix-based bioinks for enhanced mechanical integrity. *Mater Today Bio*. 2025;32:101859.

doi: 10.1016/J.MTBIO.2025.101859

104. Enayati-Gerdroodbar A, Khayati A, Ahmadi M, Pourabbas B, Ali Aboudzadeh M, Salami-Kalajahi M. An overview on potential of novel photoinitiators for vat photopolymerization-based 3D/4D printing formulations. *Eur Polym J*. 2024;221:113552.

doi: 10.1016/J.EURPOLYMJ.2024.113552

105. Deng H, Yin J, Sun Y, *et al*. Application of new photoinitiating systems based on BODIPY derivatives in long-wavelength photo-induced free radical polymerization. *Eur Polym J*. 2025;228:113833.

doi: 10.1016/J.EURPOLYMJ.2025.113833

106. Rayat Pisheh H, Hoseinian MS, Dezfoulian D, *et al*. Digital light processing bioprinting: bioink innovations and applications in tissue and organ regeneration. *J Biol Eng*. Published online July 11, 2026.

doi: 10.1186/s13036-026-00718-w

107. Jacobs PF, Reid DT. *Rapid Prototyping & Manufacturing: Fundamentals of Stereolithography*. Society of Manufacturing Engineers in cooperation with the Computer and Automated Systems Association of SME; 1992.

108. Zhu H, Yang H, Ma Y, *et al*. Spatiotemporally Controlled Photoresponsive Hydrogels: Design and Predictive Modeling from Processing through Application. *Adv Funct Mater*. 2020;30(32).

doi: 10.1002/ADFM.202000639

109. Danis K, Ilgar S, Saraj S, Topuzogullari M, Gunduz O, Ustundag CB. Influence of Light Exposure Time on the Vat Photopolymerization of Methacrylated PVA Microneedles. *ACS Omega*. 2026;11(29):44284-44293.

doi: 10.1021/acsomega.6c04499

110. Pagnotta G, Becconi M, Malferrari M, *et al*. Development of a tissue construct with spatially controllable stiffnessviaa one-step 3D bioprinting and dual-crosslinking process. *Mater Adv*. 2024;4(16):3491-3505.

doi: 10.1039/D3MA00319A

111. Sharifi S, Sharifi H, Akbari A, Chodosh J. Systematic optimization of visible light-induced crosslinking conditions of gelatin methacryloyl (GelMA). *Scientific Reports*. 2021;11(1):23276.

doi: 10.1038/s41598-021-02830-x

112. González G, Baruffaldi D, Martinengo C, *et al*. Materials Testing for the Development of Biocompatible Devices through Vat-Polymerization 3D Printing. *Nanomaterials*. 2020;10(9):1788.

doi: 10.3390/NANO10091788

113. Luo Z, Zhang H, Chen R, *et al*. Digital light processing 3D printing for microfluidic chips with enhanced resolution via dosing- and zoning-controlled vat photopolymerization. *Microsyst Nanoeng*. 2023;9(1):103.

doi: 10.1038/s41378-023-00542-y

114. Kashi PA, Bachlechner C, Huc-Mathis D, Jäger H, Shahbazi M. A porous 3D biofilm-inspired alginate/gellan hydrogel fabricated via dual-wavelength UV-crosslinking printer: Structural and rheological properties. *Carbohydr Polym*. 2025;370:124246.

doi: 10.1016/J.CARBPOL.2025.124246

115. Coser C, Ghaemmaghami AM, Yang J. Soft tissue-mimicking hydrogel stiffness modulates polarisation of human monocyte-derived macrophages. *Biomater Sci*. 2025;13(23):6637-6651.

doi: 10.1039/d5bm01187f

116. Mazzoli A, Greco S, Luzi F, *et al*. 3D-Printed Alginate-Based Hydrogels with Appropriate Rheological Properties and Efficient Development of Cell Spheroids. *Polymers 2025, Vol 17, Page 1730*. 2025;17(13):1730.

doi: 10.3390/POLYM17131730

117. Kim J, Choi YJ, Gal CW, Sung A, Park H, Yun HS. Development of an alginate-gelatin bioink enhancing osteogenic differentiation by gelatin release. *Int J Bioprint*. 2023;9(2):660.

doi: 10.18063/IJB.V9I2.660

118. Hazur J, Röder J, Czwalinna J, Schubert DW, Boccaccini AR. Pre-Crosslinking with Hydrogel Microparticles Enhances the Printability of Alginate-Based Inks. *Macromol Mater Eng*. 2023;308(12):2200675.

doi: 10.1002/MAME.202200675

119. Feng H, Song Y, Lian X, *et al*. Study on Printability Evaluation of Alginate/Silk Fibroin/Collagen Double-Cross-Linked Inks and the Properties of 3D Printed Constructs. *ACS Biomater Sci Eng*. 2024;10(10):6581-6593.

doi: 10.1021/ACSBIOMATERIALS.4C01522

120. Das S, Jegadeesan JT, Basu B. Gelatin Methacryloyl (GelMA)-Based Biomaterial Inks: Process Science for 3D/4D Printing and Current Status. *Biomacromolecules*. 2024;25(4):2156-2221.

doi: 10.1021/ACS.BIOMAC.3C01271

121. Zhu W, Ma X, Gou M, Mei D, Zhang K, Chen S. 3D printing of functional biomaterials for tissue engineering. *Curr Opin Biotechnol*. 2016;40:103-112.

doi: 10.1016/J.COPBIO.2016.03.014

122. Mao Q, Wang Y, Li Y, *et al*. Fabrication of liver microtissue with liver decellularized extracellular matrix (dECM) bioink by digital light processing (DLP) bioprinting. *Mat Sci Eng*

C-mater. 2020;109:110625.

doi: 10.1016/j.msec.2020.110625

123. Jeon O, Alt DS, Ahmed SM, Alsberg E. The effect of oxidation on the degradation of photocrosslinkable alginate hydrogels. *Biomaterials*. 2012;33(13):3503-3514.

doi: 10.1016/J.BIOMATERIALS.2012.01.041

124. Liu W, Madry H, Cucchiarini M. Application of Alginate Hydrogels for Next-Generation Articular Cartilage Regeneration. *Int J Mol Sci*. 2022;23(3):1147.

doi: 10.3390/IJMS23031147

125. Fenn SL, Miao T, Scherrer RM, Oldinski RA. Dual-Crosslinked Methacrylated Alginate Sub-Microspheres for Intracellular Chemotherapeutic Delivery. *ACS Appl Mater Interfaces*. 2016;8(28):17775.

doi: 10.1021/ACSAMI.6B03245

126. Román-Guerrero A, Cortés-Camargo S, Alpizar-Reyes E, *et al*. Chemically Modified Alginate-Based Hydrogel-Matrices in Drug Delivery. *Macromol 2025, Vol 5, Page 36*. 2025;5(3):36.

doi: 10.3390/MACROMOL5030036

127. da Silva CM, Reis RL, Correlo VM, Jahno VD. The efficient role of sodium alginate-based biodegradable dressings for skin wound healing application: a systematic review. *J Biomater Sci Polym Ed*. 2024;35(3):397-414.

doi: 10.1080/09205063.2023.2289247

128. Boddupalli A, Bratlie KM. Second harmonic generation microscopy of collagen organization in tunable, environmentally responsive alginate hydrogels. *Biomater Sci*. 2019;7(3):1188-1199.

doi: 10.1039/C8BM01535J

129. Vashishtha G, Chauhan S, Zimroz R, Yadav N, Kumar R, Gupta MK. Current Applications of Machine Learning in Additive Manufacturing: A Review on Challenges and Future Trends. *Arch. Comput. Methods Eng*. 2024;32(4):2635-2668.

doi: 10.1007/S11831-024-10215-2

130. Ma Y, Tian Z, Wang B, *et al*. Enhancing the 3D printing fidelity of vat photopolymerization with machine learning-driven boundary prediction. *Mater Des*. 2024;241:112978.

doi: 10.1016/J.MATDES.2024.112978

131. Standard Guide for Bioinks Used in Bioprinting. Published online March 15, 2024.

doi: 10.1520/F3659-24

132. Afshar AK, Mirshafiei M, Saberi A, *et al*. From light to life: Photocrosslinkable bioinks and their role in 3D bioprinting for shaping future regenerative medicine. *Bioprinting*. 2026;57:e00487.

doi: 10.1016/j.bprint.2026.e00487

133. U.S. Food and Drug Administration. Process of 3D Printing Medical Devices. Accessed July 28, 2026. https://www.fda.gov/medical-devices/3d-printing-medical-devices/process-3d-printing-medical-devices